UMN-TH-1502/96
astro-ph/9607106
July 1996

The Effects of an Early Galactic Wind on the Evolution of D, ^{3}He and Z

Sean Scully[1], Michel Cassé [2], Keith A. Olive[1], and Elisabeth Vangioni-Flam[3]

[1]*School of Physics and Astronomy, University of Minnesota Minneapolis, MN 55455, USA*

[2]*Service d'Astrophysique, DSM, DAPNIA, CEA, France*

[3]*Institut d'Astrophysique de Paris, 98bis Boulevard Arago, 75014 Paris, France*

Abstract

The predictions of the abundances of D and ^{3}He from Big Bang Nucleosynthesis (BBN) and recent observations of these two isotopes suggest the need to develop new chemical evolution models. In particular, we examine the role of an early episode of massive star formation that would induce a strong destruction of D and a galactic wind. We discuss the ability of these models to match the observed local properties of the solar neighborhood such as the gas mass fraction, oxygen abundance, the age-metallicity relation, and the present-day mass function (PDMF). We also examine in detail the ability of the chemical evolution models discussed to reproduce the apparent lack of low mass, low metallicity stars in the solar neighborhood, namely the G-dwarf distribution. Indeed, we find models which satisfy the above constraints while at the same time allowing for a large primordial D/H ratio as is reportedly measured in some quasar absorption systems at high z, without the overproduction of heavy elements. The latter constraint is achieved by employing a simple dynamical model for a galactic wind.

1 Introduction

In addition to the cosmic microwave background radiation and the Hubble expansion, another testable prediction of the standard hot big bang model is the synthesis of the light elements D, ^{3}He, ^{4}He, and, ^{7}Li (Walker *et al.* 1991). This prediction, tested against observations, is not always simple. Most of these elements undergo significant galactic processing which has changed their abundances over time. In the cases of ^{4}He and ^{7}Li, primordial values can be reasonably well determined directly from observations. ^{4}He may be inferred from low metallicity HII regions (see e.g. Pagel *et al.* 1992; Olive & Steigman 1995; Olive & Scully 1996). Observations of a uniform abundance of ^{7}Li in halo dwarfs are interpreted to be the primordial value for ^{7}Li/H (Spite & Spite 1982, Thorburn 1994 and Boesgaard 1996). Indeed, it has been argued that on the basis of these two isotopes. one can confidently constrain the single parameter (the baryon-to-photon ratio, η) of big bang nucleosynthesis (Fields and Olive 1996, Fields *et al.* 1996). On the other hand, in the cases of D and ^{3}He, one observes the present day abundances and solar abundances of these elements. Therefore, an understanding of the processes which alter the abundances of these elements over time is necessary if one is to use the observational data to constrain their primordial values as a test of BBN. The evolution of D and ^{3}He will be examined here in terms of galactic chemical evolution models.

In modeling the evolution of D/H, it is assumed that all of the observed deuterium is primordial, as stars completely destroy D in their pre-main-sequence phase. As a result, the present interstellar medium (ISM) abundances of D are depleted from their primordial values and represent firm lower bounds to the primordial abundance. The solar value of D/H can only be indirectly determined from the difference between the ^{3}He/H ratio in the solar wind (which contains ^{3}He from processed D) and in meteorites (Geiss 1993). The solar value of D/H may also be determined from abundance measurement on the surface of Jupiter (Niemann *et al.* 1996, Ben Jaffel *et al.* 1996). In addition, classical stellar models predict (cf. Iben & Truran 1978) that low mass stars are net producers of ^{3}He, but more massive stars destroy some fraction of it (Dearborn, Schramm & Steigman, 1986). Because of the pre-main-sequence destruction of D and its conversion to ^{3}He, the evolution of these two

elements is closely tied together. The amount of ^{3}He ejected from a star depends greatly on the amount of D present at its birth. Uncertainties, therefore, not only exist in the chemical evolution but above all in the stellar production of ^{3}He, as shown clearly by Schatzman (1987).

Vangioni-Flam, Olive & Prantzos (1994) explored the evolution of D and ^{3}He choosing primordial values of these elements corresponding to baryon to a photon ratio $\eta = 3 \times 10^{-10}$, a value consistent with the primordial values inferred from observations of ^{4}He and ^{7}Li and the canonical treatment of the evolution of D and ^{3}He (Walker *et al.* 1991). Using closed box models of galactic chemical evolution, they found that ^{3}He is overproduced compared with the observed solar and present-day values of ^{3}He unless it is assumed that ^{3}He is destroyed significantly in low-mass stars (ie, at levels comparable to the destruction in more massive stars). What is problematic however, is that there is strong evidence that ^{3}He is produced in low mass stars since abundances as high as ^{3}He/H $\sim 10^{-3}$ have been observed in planetary nebulae (Rood, Bania & Wilson, 1992; Rood *et al.* 1995). Including the production of ^{3}He as calculated by Iben & Truran (1978), however leads to a substantial overproduction of ^{3}He at the solar epoch (Olive *et al.* 1995, Galli *et al.* 1995, Dearborn *et al.* 1996). This problem may be remedied if ^{3}He is only produced in a narrow mass range (0.9 to 1.0 $M_\odot$), in agreement with the scarcity of ^{3}He rich planetary nebulae (Rood *et al.* 1995) and destroyed in higher mass stars as we show below. For the most part, however, we will concentrate on the evolution of D/H and the metallicity as traced by O/H and Fe/H. As shown in Scully *et al.* (1996), even in chemical evolution models with rather extreme assumptions regarding star formation rates and stellar and galactic winds, the problem of ^{3}He can not be fully resolved. Thus it seems evident a proper understanding of ^{3}He evolution requires some major modification in the stellar evolution of ^{3}He.

To make matters more difficult (from the point of view of chemical evolution), some recent observations of D/H in quasar absorption systems indicate a high primordial value around 2×10^{-4} (Carswell *et al.* 1994; Songaila *et al.* 1994), requiring destruction factors in excess of $\sim$10. There remains some reason to be cautious of the original observations because of reports of D/H an order of magnitude lower in other quasar absorption systems (Tytler, Fan, & Burles 1996, Burles & Tytler 1996). A recent re-observation of the high D/H

absorption system has been resolved in to two components, both yielding high values with an average value of D/H $= 1.9 \pm 0.4 \times 10^{-4}$ (Rugers & Hogan 1995a) as well as additional systems with a similar high value (Rugers & Hogan 1996b,c). Other high D/H ratios were reported by Carswell *et al.* (1996) and Wampler *et al.* (1996).

The cosmological consequences of a high primordial abundance of D/H was discussed by Vangioni-Flam and Cassé (1995) and by Dar (1995). Interestingly enough, in a recent analysis of the predictions of BBN neglecting the observational data on solar and ISM D and ^{3}He (justified by the current uncertainties in both the stellar and chemical evolution of these isotopes), Fields & Olive (1996) and Fields *et al.* (1996) found that the reasonably well determined abundances of ^{4}He and ^{7}Li lead to the prediction of a low value for $\eta = 1.8^{+1.0}_{-0.2} \times 10^{-10}$ which corresponds of a value of D/H $= 1.8^{+0.5}_{-0.9} \times 10^{-4}$ in excellent agreement with the quasar absorption system measurements. In contrast, the low D/H measurements, if they truly represent the primordial value are not consistent with ^{4}He or ^{7}Li unless it can be argued that the observed ^{4}He abundances are seriously underestimated and that ^{7}Li has been significantly depleted.

Large deuterium destruction factors (of order 5 – 10 from primordial values to present) in models of galactic chemical evolution were first shown to be viable by Vangioni-Flam & Audouze (1988). These models typically assumed an enhanced rate of massive star formation in the early stages of galactic evolution. However, these types of models have tended to be criticized: Reeves (1991) argued that on the basis of the nuclear chronometers, no more than a factor of 2 – 3 destruction was possible, though it was later shown in Scully & Olive (1995) that the chronometer constraints could in fact be satisfied in a large class of models which provide for significant D destruction. It is also often claimed (see eg. Edmunds 1995) that models with large D destruction factors suffer from a G-dwarf problem. We will clarify the situation with regard to the G-dwarf distribution below. For deuterium destruction factors above 10, other solutions have been proposed which invoke a galactic wind in the primitive galaxy (Vangioni Flam and Cassé 1995).

A large deuterium destruction factor requires a high degree of gas processing. This large astration could, in turn, induce an excessive metallicity in the ISM. One possibility to avoid the over-production of metals is to invoke an early galactic wind driven by supernovae (SN).

Such a wind could keep the abundance of metals down to a reasonable level in the galactic disk and at the same time remove gas from this reservoir. Furthermore, the D free ejecta of low mass, long lived stars, diluted in relatively small amounts of the ISM would induce a large decrease of the D/H ratio at late times. Thus, the evolution of both D and Z can be strongly influenced by the presence of galactic winds or outflow (Vangioni-Flam & Cassé, 1995).

The possibility of a galactic wind which is driven directly by supernovae explosions is in fact well documented (Larson 1974, Vader 1986, Charlton & Salpeter 1989, David *et al.* 1990, Wang & Silk 1993). In the following, we will couple a simple wind model inspired by Larson (1974) and David *et al.* (1990) to a chemical evolutionary code. Our criterion is the following: an early galactic wind can develop only if the supernova remnants overlap before radiatively dissipating all of their energy. This ensures an efficient conversion of the explosive supernova energy into bulk kinetic energy of the surrounding medium. The maximum mass removed per supernova (neglecting radiative losses) is that accelerated above the escape velocity, about 500 km/s in the solar vicinity, and in the most favorable conditions the galactic mass loss rate is $\sim 40\ \dot{N}_{SN}\ \mathrm{M}_{\odot}$, where $\dot{N}_{SN}$ is the rate of core collapse SN.

To produce the outflow and the desired destruction of D, it is necessary to choose an IMF which is skewed toward producing more massive stars, especially at early times. These models have the advantage of quickly ejecting large amounts of D and ^{3}He free material and are able to generate winds in favorable conditions. However, producing more massive stars will lead to generous heavy element production. In particular, since these stars are the primary producers of ^{16}O and produce a large amount of ^{56}Fe as well, including more of these stars will lead to an overproduction of these elements. Galactic winds of the type discussed above is a way to reduce or remove the overproduction of metals in these models.

Changing the IMF in favor of more massive stars may lead to a discrepancy between the predicted and observed PDMF (see e.g. Scalo 1986). As a result, we consider the possibility that more massive stars were formed early on in galactic history while star formation today matches a more normal IMF. A class of models have been proposed in which the star formation is bimodal (see e.g. Larson, 1986; Wyse and Silk, 1987; Vangioni-Flam and Audouze, 1988; François et al. 1990). In these models, the formation of more massive stars in the

early history of the galaxy is super-imposed over a standard formation rate ($\propto$ the gas mass fraction). These models were proposed originally to fit the G-dwarf distribution in the disk (Larson 1986; Olive 1986), since it is equivalent to a prompt initial enrichment (PIE) (Truran & Cameron 1971, Talbot & Arnett 1973). These models are found to be consistent with the Scalo (1986) PDMF. We will explore these models to reconcile the high D destruction with the solar metallicity .

We shall begin by describing in section 2 our basic chemical evolution model and how the wind affects the evolution of D, ^{3}He, and the heavy elements. In section 3, we summarize the models we will be presenting. Section 4 is devoted to discussing the ability of these models to match the local observed properties.

2 Chemical Evolution Models

2.1 Basic Equations

A basic review of chemical evolution models can be found in Tinsley (1980). We adopt her notation in the following discussion. In our models, we consider the actual stellar lifetimes thus avoiding the instantaneous recycling approximation (IRA). We shall be comparing the results of our models to the observed values of the light elements in the solar system and local ISM. Thus we restrict our calculation to the solar neighborhood.

Chemical evolution models stem from tracing the evolution of the gas mass in the disk of the galaxy. In this study, we will consider only the effects of gaseous flows out of the disk. Thus the equation for the gas mass is given by

$$\frac{dM_G}{dt} = -\psi(t) + e(t) - o(t) \tag{1}$$

In this equation, $\psi(t)$ is the rate at which gas is being used up by star formation. The rate of outflow of gas from the disk, $o(t)$, will be determined by our galactic wind model and will be discussed in detail in section 2.2 below. The rate at which gas is returned to the ISM by mass loss or stellar deaths either in supernova events or in planetary nebulae, $e(t)$, is given

by

$$e(t) = \int_{m_1(t)}^{m_{up}} (m - m_R)\varphi(m,t)\psi(t - \tau(m))dm, \tag{2}$$

where $m_1(t)$ is the mass of a star which dies at age t, and m_{up} is the upper mass limit of stars which will supernova. $\tau(m)$ is the main sequence lifetime of a star of mass m. Stellar lifetimes are adopted from Scalo (1986). m_R is the mass of the left over remnant (white dwarf, neutron star or black hole). In our calculations, m_R is taken to be (Iben & Tutukov, 1984),

$$m_R = 0.11m + 0.45M_\odot \quad m \leq 6.8M_\odot, \tag{3}$$

$$m_R = 1.5M_\odot \quad m > 6.8M_\odot. \tag{4}$$

The IMF, $\varphi(m,t)$, is allowed to be both a function of mass and time and is normalized such that

$$\int_{m_{low}}^{m_{end}} m\varphi(m,t)dm = 1. \tag{5}$$

In this equation, m_{end} is the upper mass limit of stars which can form. In principle, there could be a distinction between m_{end} and m_{up} in these equations. It has been suggested (Larson 1986, Olive *et al.* 1987) that one way to avoid the overproduction of ^{16}O in chemical evolution models is to limit the upper mass limit size of stars which supernova. Stars more massive than this are assumed to collapse entirely into black holes returning no material to the ISM. However, in bimodal models with a rapidly decreasing SFR, m_{up} is required to be low (around 16 $M_\odot$ in some cases). Because we ascribe a physical mechanism to a galactic wind (as opposed to a low m_{up}), we will set $m_{up} = m_{end}$ and concentrate on the galactic wind.

In what follows, we assume bimodal star formation in most cases. We adopt models similar to those in Vangioni-Flam & Audouze (1988) and François, Vangioni-Flam and Audouze (1990).

2.2 Galactic winds and chemical evolution

In this subsection, we outline the calculation of the abundances of the elements including the effects of outflow. We consider in our models supernova-driven winds. Our aim is to find

a simple scheme to couple a wind prescription to a galactic evolutionary model, as has been done for elliptical galaxies (Larson 1974, Vader 1986, David *et al.* 1990, Elbaz *et al.* 1995). An early wind, indeed, could offer a possible way to explain large D destruction without metal overproduction. At the beginning of the evolution, the wind removes a significant part of the galactic gas, ejecting from the galactic disk freshly synthesized elements. Much later, the D free ejecta of low mass stars are diluted in relatively smaller amounts of disk material.

Note that if we use a rate of gas loss of the form $dM/dt = -\alpha\psi$, where α is constant, we recover the Hartwick (1976) solution : $Z = y/(1+\alpha)$ in the IRA where Z is the final mean metallicity and y is the yield. Indeed, this "reduced yield" would moderate the metal production (see also Wang and Silk 1993). The constant α depends on the escape velocity of the galaxy, the fraction of gas mass converted to stars (which in turn depends on the IMF), and the fraction of the total supernova energy which is available for heating the gas to escape velocity and depends of the radiative losses of SNR. The cooling rate is a sensitive function of the temperature, so that for $T < 5 \times 10^6$K, radiative losses are large and lead to thermal instabilities. The Galaxy is presently in this regime.

We consider a model similar to that of Vader (1986) in which continuous gas loss from the disk is established. We assume that some fraction, ϵ, of the supernova energy goes into heating the ISM gas to the escape velocity for the disk and subsequently leaves the system. The rate at which mass is lost from the system is given by

$$\dot{M}_W = \frac{2\epsilon E_{SN} \dot{N}_{SN}}{v_{esc}^2}, \tag{6}$$

where $\dot{N}_{SN}$ is the supernovae rate,

$$\dot{N}_{SN} = \int_8^{m_{up}} \varphi(m,t)\psi(t)dm. \tag{7}$$

We assume that all stars of mass greater than 8 $M_\odot$ will supernova. E_{SN} is the amount of energy released per supernova which we will assume to be 10^{51} ergs. The escape velocity, v_{esc}, in the solar neighborhood is of the order twice the rotational velocity i.e. $\sim 500\text{kms}^{-1}$ including the dark matter halo (otherwise it would be about 300 kms^{-1}). We shall assume

that the escape velocity has not changed significantly over the history of the galaxy in spite of the mass loss due to the wind since dark matter dominates the gravitational potential of the Galaxy.

Radiative losses from the SNRs become significant if cooling begins before the SNRs collide and merge with one another. We want to estimate the fraction, ϵ, of the initial supernova energy available for heating the ISM gas to escape velocity. We consider first the criteria for when radiative cooling becomes important. In order for supernova remnants to overlap before cooling, David et al (1990) have determined a critical supernova rate $\dot{N}_{crit}$ which the actual supernova rate must exceed,

$$\dot{N}_{crit} = 0.83 \mathrm{kpc}^{-3} \mathrm{yr}^{-1} (\frac{n}{\mathrm{cm}^{-3}})^{1.82}. \tag{8}$$

If the supernova rate exceeds this value then no cooling of the outer shell has occurred before remnants collide leaving the entire energy of the supernova explosion available to heat the gas. In the models we consider below, $\dot{N}_{SN} < \dot{N}_{crit}$ and $\epsilon < 1$. To compare $\dot{N}_{SN}$ and $\dot{N}_{crit}$, we scale the SFR rate to 3 $\mathrm{M}_{\odot}/\mathrm{pc}^2/\mathrm{Gyr}$ (Tinsley 1980) and assume a scale height of 400 pc (Rana 1991).

If cooling is important, the outer shell of the SNR will dissipate its thermal energy very quickly contributing no energy to drive a galactic wind. The only source for wind energy is then the thermal energy of the hot interior of the remnant. Larson (1974) has estimated the residual thermal energy of a SNR when it collides and merges with other remnants in terms of the supernova rate and critical supernova rate,

$$E_r \sim 0.22 E_{SN} (\frac{\dot{N}}{\dot{N}_{crit}})^{0.32}. \tag{9}$$

Thus the fraction of energy available to drive the galactic wind, ϵ, is given by

$$\epsilon = 0.22 (\frac{\dot{N}}{\dot{N}_{crit}})^{0.32}. \tag{10}$$

When the disk of the Milky Way was young, the gas mass fraction was larger by a factor of about 10, the scale height of the gas was probably much higher than it is now (say 1 kpc),

and the radius of the disk was possibly larger. We estimate then that the initial gas density was perhaps 5 to 10 times greater than it is today. To determine the number density of gas at previous times, we scale the number density with the evolution of the gas mass fraction. We choose a density of the form

$$n = (\frac{\sigma}{0.1}) n_{today}, \tag{11}$$

where the number density today in the solar neighborhood is 0.5 cm^{-3}.

Since we shall be considering bimodal models where the supernova rate is much higher in the past than it is today, the possibility exists that more gas than can be swept up by a SNR can be heated to the escape velocity. Thus we need to impose this constraint on our mass loss mechanism. The shell radius at which cooling becomes significant is given by (Larson 1974),

$$R_c = 27 n^{\frac{-7}{17}}, \tag{12}$$

Thus the amount of mass that can be swept up by a SNR is

$$M_s = \frac{4}{3}\pi\rho R_c^3 = 1859 n^{\frac{-4}{17}}. \tag{13}$$

In reality, we should choose the radius not at which cooling becomes important but rather the radius at which SNRs collide which is somewhat larger. In practice, however, we find that M_s is much larger than the mass which can be heated to escape velocity at all times.

Vader (1986) demonstrated that simple supernova-driven wind models with a homogeneous ISM cannot reproduce the observed chemical properties of dwarf elliptical galaxies and proposed metal enhanced galactic wind models. If some fraction of supernovae ejecta which power the galactic wind do not cool radiatively and is flushed directly out of the galaxy, it will play no role in the chemical enrichment of the ISM. The remaining fraction leads to an effective yield $y(1-\nu)$ for galactic chemical evolution. Thus Vader's models relied on two parameters: the efficiency ϵ which we take from Eq. (10), and the the fraction of the metals produced in the supernova progenitors which is blown out of the galaxy, ν, which we will adjust to match the observed metallicity in the solar neighborhood. In our most extreme cases, we take ν to be ~ 0.8, which is to be compared with 0.9 in Vader's models.

We can now describe how we implement these mechanisms for galactic winds. It is convenient to rewrite the mass ejected from stars $e(t)$ as the sum of the mass ejected in supernova events, $e_s(t)$, and the mass ejected by all other stars $e(t) - e_s(t)$. Thus the rate of mass which outflows from the disk is a combination of the mass lost in the winds, $\dot{M}_W$, and the fraction of the supernova ejecta which leaves the disk, $\nu e_s(t)$. Equation (1) may now be rewritten as

$$\frac{dM_G}{dt} = -\psi(t) + e(t) - \nu e_s(t) - \dot{M}_W, \tag{14}$$

and

$$o(t) = \nu e_s(t) + \dot{M}_W \tag{15}$$

Equation (14) may then be extended to solve for the time evolution of the mass fraction of a heavy element, X:

$$\frac{d(XM_G)}{dt} = -\psi(t)X + e_X(t) - \nu e_{sX}(t) - \dot{M}_W X, \tag{16}$$

where $e_X(t)$ and $e_{sX}(t)$ represent the total amount of metals ejected by stars and the type II supernova contribution respectively. Equation (16) can be further simplified to read

$$\frac{dX}{dt} = \frac{(\nu e_s(t) - e(t))X - \nu e_{sX}(t) + e_X(t)}{M_G} \tag{17}$$

We use this equation to calculate the abundances of the elements such as ^{16}O (For D, $e_{\rm D}(t) = 0$ since D is totally destroyed in stars.) We have adopted the yields of Woosley & Weaver (1995) for ^{16}O. For Fe, we include contributions from both type I and II supernovae. We take the type II yield from Woosley & Weaver (1995). For type I supernovae, we take the yield to be 0.7 $M_\odot$ (Thielemann, Nomoto, & Yokoi 1986) for stars between 1.5 and 8 $M_\odot$ and we fix the rate of type I events to obtain a maximum iron abundance which can be compared with the G-dwarf data below. In order to reproduce observational features such as the evolution of [O/Fe] verses [Fe/H] we have built in to our models a 1 Gyr time delay corresponding to the lifetime of the progenitors of type I supernovae (see e.g. Yoshii *et al.* 1996). (Note that the Woosley & Weaver (1995) iron yields are somewhat high and give a low value for [O/Fe] vs. [Fe/H] at very low metallicity (see eg. Matteucci & François 1989).)

2.3 D and ^{3}He

Our goal in this subsection is to outline the evolution of D and ^{3}He. We begin by summarizing the observational constraints on these elements. As discussed above, detections of D using quasar absorption systems have been reported recently. The high values of D/H determined in these systems are ideal for demonstrating the effects of outflow. In models where significant D destruction is required, the stellar processing which destroys D, produces heavy elements whose abundances can be controlled by outflow. In these cases we take the primordial D/H abundance to be 2×10^{-4}. As we noted above, these measurements are still controversial and we will also show results based on a somewhat lower value which is still consistent with ^{4}He and ^{7}Li, $(\mathrm{D/H})_p = 7.5 \times 10^{-5}$ a value already high from the perspective of evolution and high enough to demonstrate the effects of outflow that we wish to explore. For completeness, we also consider a low value for D/H = 2.5 $\times 10^{-5}$ as inferred in some observations of quasar absorption systems.

The present day D abundance has recently been determined by Linsky *et al.* (1993, 1995) using the HST. They determined an ISM D/H abundance of

$$(\mathrm{D/H})_{\mathrm{ISM}} = 1.60 \pm 0.09^{+0.05}_{-0.10} \times 10^{-5} \tag{18}$$

The present day ^{3}He abundance has been determined in a number of galactic HII regions (Balser *et al.* 1993). These values range from $1.1 - 4.5 \times 10^{-5}$. A recent measurement of ^{3}He/H by the Ulysses satellite by Gloeckler and Geiss (1996) in low energy ions filtering from the local interstellar medium in the solar cavity, has been performed finding

$$(^3\mathrm{He/H})_{\mathrm{ISM}} = 2.2^{+0.7}_{-0.6} \pm 0.2 \times 10^{-5} \tag{19}$$

and is complementary to the local D/H measurement. We will take this measurement as a reference for the present and local galactic environment.

The presolar D and ^{3}He abundances were recently reviewed in Geiss (1993) and discussed in Scully *et al.* (1996). Presolar D is not directly measured. Instead, a comparison is made between the ^{3}He abundance measured in the low temperature components of carbonaceous chondrite meteorites (which are in good agreement with the measured ^{3}He/H ratio in the

lunar soil and solar wind) and the abundance measured in high temperature components these meteorites. The latter ^{3}He measured in the carbonaceous chondrites represents a true presolar abundance for this element. Since it is assumed that all of the D present in the gas from which a star is formed is converted to ^{3}He in the pre-main sequence phase, the other measurements really represent D + ^{3}He present before the formation of the solar system. Our adopted presolar values of D, ^{3}He, and D + ^{3}He are (Scully *et al.* 1996):

$$[(D +^3 He)/H]_\odot = (4.1 \pm 0.6 \pm 1.4) \times 10^{-5}, \tag{20}$$

$$(^3He/H)_\odot = (1.5 \pm 0.2 \pm 0.3) \times 10^{-5}, \tag{21}$$

$$(D/H)_\odot = (2.6 \pm 0.6 \pm 1.4) \times 10^{-5}. \tag{22}$$

However, recent measurements of surface abundances on Jupiter show a somewhat higher value for D/H, D/H $= 5 \pm 2 \times 10^{-5}$ (Niemann *et al.* 1996) and D/H $= 5.9 \pm 1.4 \times 10^{-5}$ (Ben Jaffel *et al.* 1996). If these values are confirmed and if fractionation does not significantly alter the D/H ratio (as it was suspected to for previous measurements involving CH_3D), they should be taken into account in galactic chemical evolution models. As it stands, these values are marginally consistent with the *inferred* meteoritic values. In a chemical evolution model, they can be made consistent with the high QSO absorber D/H values, but not the low ones which would then require the net production of D/H.

The evolution of D in the ISM can be determined by extending equation (16),

$$\frac{d(M_G D)}{dt} = -\psi(t) D - \dot{M}_W D. \tag{23}$$

By substituting equation (14) into the above equation and with further simplification, the D evolution is governed by,

$$\frac{dD}{dt} = \frac{(\nu e_s(t) - e(t))D}{M_G}. \tag{24}$$

More complicated than the history of deuterium is that of ^{3}He. In more massive stars ($M < 5 - 8 M_\odot$) , ^{3}He is destroyed on average (although not completely). In lower mass stars ($1\ M_\odot \leq M \leq 2 M_\odot$), it is likely that ^{3}He is produced. Iben and Truran (1978) estimate the

^{3}He in the surface layers of stars $< 8M_\odot$ to be

$$(\frac{^3He}{H}) = 1.8 \times 10^{-4}(\frac{M_\odot}{M})^2 + 0.7[\frac{(D +^3 He)}{H}]_i \tag{25}$$

where the bracketed term is the contribution from the D in the pre-main sequence phase. Similarly, significant production of ^{3}He was found by Vassiladis & Wood (1993) and by Weiss, Wagenhuber, and Denissenkov (1995). There is in addition, some observational support for the production of ^{3}He in low mass stars as evidenced by the high ^{3}He/H ratios measured in planetary nebulae (Rood, Bania & Wilson 1992, Rood *et al.* 1994).

There has been a considerable amount of discussion recently concerning the ^{3}He production in low mass stars. It has been argued (Charbonel 1994, 1995, Hogan 1995, Wasserburg, Boothroyd, & Sackman, I.-J. 1995, Weiss *et al.* 1995, Boothroyd & Sackman 1995, Boothroyd & Malaney 1995) that perhaps low mass stars in the range 1–2 $M_\odot$ are in fact net destroyers of ^{3}He. As it appears unlikely that chemical evolution alone can resolve the problem concerning the overproduction of ^{3}He (Scully *et al.* 1996), these latter yields for low mass stars should be taken seriously. For larger mass stars, we adopt the ^{3}He survival fraction given by Dearborn, Schramm, & Steigman (1986) which is consistent with the recent results of Woosley & Weaver (1995). The ^{3}He evolution may now be determined by following the prescription of equation (17). We will consider an alternative approach to ^{3}He in §5.

3 Models

We will consider a model with a bimodal star formation rate which includes the galactic wind described in section 2.2. The specific model has been chosen to satisfy observational constraints on D for the solar epoch and present day (we will consider different primordial values of D/H which thus affects the parameters of the model). The parameter ν is adjusted to reproduce the observed solar ^{16}O abundance. We also consider only models which can reproduce a gas fraction today in the range of $\sigma = 0.05 - 0.20$ which roughly corresponds to the observed gas fraction (Rana 1991).

The first case we consider has a primordial D/H $= 2\times10^{-4}$ and is clearly the most extreme case in terms of the degree of D destruction. The bimodal star formation rate includes a

rapidly decreasing exponential SFR associated with an IMF favoring more massive stars which is superimposed on top of a SFR proportional to the gas mass associated with a more normal IMF. This model which we will refer to as model Ia is similar to model IV of Vangioni-Flam and Audouze (1988). The exponential component includes a SFR $\psi_2(t) = 0.29e^{-t/2}$ with an IMF $\phi(m) \propto m^{-2.7}$ in the mass range of $2 \leq m/M_\odot < 100$. The more normal component has a SFR $\psi_1(t) = 0.29M_G$ with an IMF $\phi(m) \propto m^{-2.7}$ in the mass range of $0.4 \leq m/M_\odot < 100$. We find that about 81% of the supernova ejecta or $\nu = 0.81$ is necessary to reproduce the observed solar oxygen abundance. This is to be compared with values as large as 0.9 found by Vader (1986).

As we indicated earlier, the type I to type II supernova rate is determined by the produced iron abundance in the model. In fact, the iron abundance depends on three quantities, the type I iron yield, the fraction of stars becoming type I supernovae, and the fraction of type I ejecta expelled in winds. The latter need not be equal to ν which corresponds to the type II fraction ejected. Our models rely only on the product of all three of these parameters. In model Ia, the present type I to type II SN ratio (when we refer to this ratio, we will always be referring to its present-day value) is low (2%) if we assume that no type I ejecta is expelled, whereas the ratio is 12% if we assume that winds carry the same fraction of type I ejecta as for type II. The fact that this ratio is low also reflects the high Fe yields for type II SNe from Woosley & Weaver (1995). Note that the type I to type II SN ratio should be in the range of 10 – 20 % to be consistent with observations (Tammann 1994).

When we consider the G-dwarf distribution, we will compare the above model to one in which the massive star component is followed by the more normal component sequentially. For this model we consider an exponential SFR $\psi_2(t) = 0.19e^{-t/1}$ for $t \leq 1$ Gyrs with the same massive IMF as model Ia and a SFR $\psi_1(t) = .73e^{-t/2.5}$ for $t > 1$ Gyrs with the same normal mode IMF as model Ia. In this case, we find that a value of $\nu = .68$ is necessary to reproduce the observed solar oxygen abundance. The SN I to SN II ratio in this model is 4% but can be as large as 13%. We will refer to this case as model II.

In Scully *et al.* (1996) we also considered a model in which the IMF is a function which varies in time (metallicity)

$$\varphi(m,t) \propto m^{-(1.25+O/O_\odot)}. \tag{26}$$

The dependency of the IMF on the oxygen abundance was chosen so that the oxygen abundance history predicted by the model closely matches the observations. This model was coupled to outflow with the expressed purpose of reducing the the abundance of ^{3}He. While it alleviated the problem somewhat, ^{3}He was nevertheless overproduced resulting in the conclusion that chemical evolution alone could not suffice in resolving the ^{3}He problem. The wind model here was not "designed" to fix ^{3}He and in fact because of large portions of ISM are blown out the ^{3}He abundance actually increases when outflow is included. Overall, this type of model (with the time varying IMF) does not give qualitatively different results.

We also consider models which require far less destruction of D/H. For a primordial value D/H $= 7.5 \times 10^{-5}$, we have in model Ib, a SFR, $\psi_1(t) = 0.28 M_G$ and $\nu = 0.55$. In this case the SN I to SN II ratio is only $3 - 7$ %. This is not a bimodal model. The same IMF as in the normal mode in model Ia was used. The associated ^{4}He and ^{7}Li abundances predicted by BBN are consistent with their observationally determined values. Finally for completeness, we considered a model Ic, in which the primordial D/H was set to 2.5×10^{-5}. In this case, we ran a model with a simple constant SFR, $\psi = 0.07$. This value of ψ is chosen to obtain a suitable evolution of D/H. Because heavy element *pro*duction rather than over-production is a problem, $\nu = 0$. In this case, the lower mass limit in the IMF was lowered to 0.2 $M_\odot$ and the SN I to SN II ratio is 1%. Once again, this low ratio reflects the high type II iron yields. Recall that this ratio could be adjusted upward by lowering the assumed type I yield. This value of D/H was chosen to correspond to the low D/H observed in certain quasar absorption systems (Tytler, Fan, & Burles 1996, Burles & Tytler 1996). However, it should be noted that the predicted ^{4}He and ^{7}Li abundances are not in agreement with the observations.

4 Observational Constraints and Results

4.1 Element Abundances

In figure 1, we show the evolution of D/H as a function of time for model Ia along with the evolution of ^{3}He/H. This model is capable of adequately explaining the evolution of D/H even with the high primordial abundance of D/H $= 2.0 \times 10^{-4}$. Figure 2 illustrates the

corresponding oxygen evolution for model Ia which we use as a tracer for heavy element production. In both figures 1 and 2, the dotted line shows the evolution of a closed box model (no outflow) with the SFR and IMF of model Ia, the solid line in contrast shows the effect of the galactic winds as described in section 2.2. With the inclusion of a metal enriched galactic wind, we are able to find models which can destroy a sufficient amount of D without overproducing metals. The present gas mass fraction in this model is 0.07 (it turns out to be between 0.07 and 0.10 in all of the models considered). Figures 1 and 2 also show the resulting evolution of model II.

With the D destruction necessary for our models to reproduce the observed solar and present-day D abundances, it is not surprising that if we take the Iben & Truran (1978) yields for ^{3}He, we find a a solar ^{3}He abundance of about ~ 10 times higher than is observed. Enriched outflow makes the problem worse with regard to ^{3}He. A comparison of model Ia without outflow is also illustrated on figure 1. ^{3}He increases more rapidly with outflow than without. This is because we are including in our wind a fraction of the supernova ejecta which is depleted in ^{3}He relative to the ISM abundance. There is therefore less ^{3}He poor gas available to dilute the ISM. We will discuss ways of resolving this problem in §5 below.

In figures 3 and 4, we compare the results of the three cases with differing initial D/H. In model Ib, which results in a very similar evolution to the model considered in Olive *et al.* (1995), ^{3}He is still greatly overproduced. In Ic, where the D/H abundance starts out very low, ^{3}He is consistent within the errors if systematics are included. The abundance of ^{3}He at the solar epoch is $^3\mathrm{He/H} = 2.0 \times 10^{-5}$ which is to be compared with the solar value in Eq.(21). We point out however that this is not an entirely acceptable model. First, we still destroy a bit too much deuterium. This could be fixed by including some primordial infall. However, infall would aggravate both the slightly low metallicity (we do not quite achieve solar metallicity at the solar epoch) and the somewhat high present day gas mass fraction (28%). Primordial, D-rich infall would further lower the metallicity and increase the gas mass fraction.

A considerable amount of enriched material is expelled from the galaxy in this type of model (Ia). This could contribute to the enrichment of the extra-galactic gas with heavy elements. The same process is strengthened in clusters of galaxies where ellipticals are

dominant and provide most of the metals to the intracluster gas (Elbaz *et al.* 1995) as observed by X-ray satellites (Mushotzky *et al.* 1996, Loewenstein & Mushotzky 1996). An overall metallicity of about 0.1 – 0.2 $Z_{\odot}$ results in the gas surrounding the galaxy from the enriched outflow of model Ia. Thus we can conclude that these models do not expel an unreasonable amount of metals from the Galaxy.

The amount of outflow, $o(t)$, as defined in equation (15), produced by supernovae driven winds is shown as a function of time in figure 5 for model Ia, b, c, and II. As it is directly tied to the supernova rate, it is a sharply decreasing function of time. In figure 6, the effect of outflow on the mass of Galaxy is shown. Despite the large SFR early on and the degree of D destruction in the model, the mass of the Galaxy only changes by about 30% in Ia, by 8 % in Ib and less than 3% in Ic. In model II, the mass changes by about 14%.

4.2 The G Dwarf Distribution

The distribution of G-dwarf stars as a function of metallicity serves as a constraint for chemical evolution models. G-dwarfs have sufficiently long lifetimes so that most of them which formed early on in the galaxy should be present today. The problem as normally stated is that there is a lack of metal-poor stars observed relative to the predictions of simple closed-box chemical evolution models. A number of solutions including a prompt initial enrichment (PIE) (Truran and Cameron 1971), inflow of processed material (Ostriker and Thuan 1975), and accretion of unprocessed material (Larson 1972) have been proposed. Any realistic model of the chemical evolution in the solar neighborhood should account for the lack of metal poor dwarf stars.

The rate of formation of G-dwarf stars is given by

$$\frac{dN}{dt} = \int_{m_l}^{m_h} \varphi(m)\psi(t)dm, \tag{27}$$

where $m_l = 0.8\mathrm{M}_{\odot}$ and $m_h = 1.1\mathrm{M}_{\odot}$ are the lower and upper mass limits of G-dwarf stars formed at time t. Bazan and Mathews (1990) point out that some of the G-dwarfs which formed early on would have had short enough lifetimes that they would not be present today. In order to account for this, the number of G-dwarf stars which have formed must further

be multiplied by the fraction of those which survive given by

$$f(t_g - t) = \int_{m_l}^{m(T_G - t, Z(t))} \varphi(m) dm / \int_{m_l}^{m_h} \varphi(m) dm, \tag{28}$$

where $m(T_G - t, Z(t))$ is the largest star of metallicity $Z(t)$ which is left after a time $T_G - t$.

Before we discuss the distribution of G-dwarfs for the chemical evolution models we consider, we first note the effect of (dropping) the IRA. In figures 7-9, we compare a simple closed box model with and without the IRA. In figure 7, we show the cumulative number of G-dwarfs as a function of metallicity taken here to be [Fe/H] (scaled by the Fe abundance at $t = 14$ Gyr). The data represented by points are taken from Pagel (1988). The curves show the G-dwarf totals using a simple closed-box model with $\psi = 0.25\sigma = 0.25 M_G$ and an IMF $\varphi(m) \sim m^{-2.7}$ in the range $0.4 \leq m/M_\odot \leq 100$ with (dashed) and without (solid) the IRA. There is a significant difference here which can be explained. In figure 9, we show the age metallicity relation for the two cases described above. In the IRA, the metallicity increases linearly with time, and as such a given metallicity bin corresponds to a relatively small time bin, so that at late times the product of a diminishing SFR and a small integration time produces few G-dwarfs. When the total number of G-dwarfs is normalized to the observed total (132 in this case), we see an excess at low metallicity. This is the classic G-dwarf problem. When the IRA is dropped, the Fe/H is no longer linear in time and the age-metallicity curve flattens toward higher metallicity corresponding to late times. This is due to the non-negligible lifetimes of lower mass stars, whose ejecta at late times dilutes the metallicity. As a result, the high metallicity bins correspond to significantly large time bins, and many more G-dwarfs are computed to be produced at higher metallicity. Because we normalize to the same total number of dwarfs, there are far fewer formed at early times or low metallicity. Thus the problem is shifted to a deficiency of G-dwarfs at intermediate metallicities (around [Fe/H] ≈ -0.5) and an excess at near solar metallicity. This problem is evidenced in the models of Timmes, Woosley & Weaver (1995) where the IRA is not employed.

Pagel (1988) advocates that in addition to the cumulative number of G-dwarfs it is useful to plot the change in the number of dwarf stars as a function of metallicity. Hereafter, we will refer to this as the differential G-dwarf problem. In figure 8, we show the differential

distribution of G-dwarfs vs [Fe/H] for the simple closed box model with and without the IRA. Typical errors in the data are $\sqrt{\Delta N}$ for the number of dwarfs in each bin and 0.1 dex in [Fe/H]. Again we see clearly the shift in the excess number of dwarfs to higher metallicity. In addition, notice that the turnover at higher metallicities is absent when the IRA is dropped. We conclude that any attempt to resolve the G-dwarf problem can not be based on the IRA.

In figure 10, we show the G-dwarf predictions from the bimodal models Ia, and II and model Ic. The curve for Model Ib looks very similar to that of Ic and is not shown. It is demonstrated that the models which include more massive star production at earlier times predict an abundance of metal poor stars which is more consistent with the observations. This is a result of the rapid rise of the metallicity of stars due to the rapid production of heavy elements associated with the massive star production. However, with the exception of model II (which was constructed to produce a G-dwarf distribution which more closely matches the observations), these models show a deficiency of dwarf stars at metallicities a factor of 2-3 below solar. This is the same problem witnessed in the closed box models when the IRA was dropped

Figure 11a shows the differential G-dwarf distribution for models Ia, c and figure 11b shows the result for model II. For all of the models considered, we find that there is no (or very little) excess of G-dwarfs at low metallicity. In contrast, we see clearly from the differential distribution that with the exception of model II, models Ia, and c show a deficit of dwarfs at metallicities somewhat below solar and an excess at metallicities just above solar (model Ib is similar). Thus contrary to what is often claimed, the G-dwarf distribution has very little to do with the total amount of astration of deuterium. Large deuterium destruction factors can not be excluded on this basis. It should be noted that discrepancies in the highest of the metallicity bins may be artificial. The data (Pagel 1988) show 7 out of 132 stars in the final bin at [Fe/H] between 0.1 and 0.2. We have tuned these models by adjusting the rate of type I supernovae and produced a turn over in the final metallicity bin. As in the case of the closed box models, these models result in an oxygen abundance as a function of time which flattens out after a sharp rise (figure 6). This makes for a bin size for metallicities of around solar which cover several billions of years. Thus even though the SFR is lower at these times, it is more than compensated for by the longer time period

for the formation of G-dwarfs. Thus the rise in the number of G-dwarfs towards higher metallicities. Aside from the turn over at higher than solar metallicities, these distributions are qualitatively similar to the the distribution shown in Timmes, Woosley & Weaver (1995). Model II does not exhibit this problem due to the rapidly decreasing SFR (exponential with a time constant of 2.5 Gyr). As demonstrated in François *et al.* (1990), the sequential model is best suited for obtaining an acceptable G-dwarf distribution as the massive mode in this case acts as a PIE. In this case, during the first 1 Gyr, there is significant metal production, bringing [Fe/H] close to -1.0 without the production of any dwarf stars. The "normal" mode is then shifted towards higher metallicity.

We have also checked the white dwarf production rates and accumulated white dwarf surface density for model II. If we define the white dwarf birth rate by

$$B_w(t) = \int_{m_1(t)}^{m_w} \phi(m)\psi(t-\tau(m))dm \tag{29}$$

where m_w is the upper mass limit for the formation of a white dwarf, taken here to be 8 $M_\odot$. The present white dwarf birth rate in model II is 1.4 $\times 10^{-3}$ pc^{-3} Gyr^{-1}, consistent with the rate found by Weidemann (1977). The total integrated surface density of white dwarfs is 9 $M_\odot$ pc^{-2} and is somewhat smaller than the white dwarf density found in Larson's (1986) bimodal models. Finally, the white dwarf luminosity function $n = B_w(t-t_c)\Delta t_c/2\langle z\rangle$, where t_c is the cooling time (taken from Iben and Tutukov (1984)) Δt_c is the time to cool from $M_{\rm bol} - .5$ to $M_{\rm bol} + .5$, and $\langle z\rangle$ is the scale height. In model II, the luminosity function is somewhat high at very low luminosity, n appraoches 10^{-2} pc$^-3$ mag^{-1} at $M_{\rm bol} = 17$ though it is lower than that predicted in Larson's (1986) model (Olive 1986).

Finally, in figure 12, we show the age metallicity relation for the models discussed above and compare it to the data of Edvardsson *et al.* (1993). As one can see, all of our models are well within the established scatter in the observations. Indeed, from the data on the [Fe/H] vs age, it is clear that the Galactic metallicity remains rather flat (at about solar metallicity) for most of the history of the Galaxy (the last 10-12 Gyr). The large integration time for the production of dwarf stars at solar metallicity, makes it difficult to reconcile the large number of G-dwarfs observed around [Fe/H] = -0.5, where the integration time is relatively short. This can only be done in models in which the star formation rate is a

steeply decreasing function of time. We emphasize again that this problem is very different from what is commonly referred to as the G-dwarf problem. Dropping the IRA, is nearly sufficient for resolving the problem of an excess number of dwarfs at low metallicity.

4.3 The PDMF

The only direct observational constraint on choosing an IMF is the present-day mass function (PDMF). The PDMF refers to those stars on the main sequence which are still observable today. The PDMF has been estimated from the luminosity function by Scalo (1986). We shall adopt his results for comparison with our models.

For stars which are born and have lifetimes greater than the age of the galaxy or roughly masses $< 0.9M_{\odot}$, the IMF and PDMF are directly comparable. All of these stars with lifetimes, T_m, are still on the main sequence so the PDMF, φ_{MS}, for these stars is just the total number born given by

$$\varphi_{MS} = \int_0^{T_G} \varphi(m,t)\psi(t)dt \qquad T_m \geq T_G, \tag{30}$$

where T_G is the age of the disk and T_m is the main sequence lifetime of a star of mass m. For stars more massive than this, the PDMF represents the number of stars of a given mass which have not yet evolved off of the main sequence. Thus only those stars born in the last T_m years will be on the main sequence. Therefore, the PDMF for these stars is given by

$$\varphi_{MS} = \int_{T_G - T_m}^{T_G} \varphi(m,t)\psi(t)dt \qquad T_m < T_G. \tag{31}$$

We have chosen a simple power law IMF for model Ia with $\varphi \propto m^{-2.7}$ consistent with the Scalo PDMF with some simple assumptions about the SFR (Olive *et al.* 1987). We do include a massive star component in these models but in each case the massive component steeply decreases very early on. We therefore expect that the increased production of massive stars early in the galactic history will have no effect on the PDMF predicted by these models since the larger number of massive stars created early on would have long since died out. Figure 13 shows the PDMF plotted along with the data from Scalo (1986). The PDMF predicted from the models is in good agreement with the Scalo data for stars $> 0.9M_{\odot}$. The

low mass end of the PDMF could be fit by a multislope IMF, which flattens out at low masses. This would have no effect on the issues considered here, as the only stars which affect the chemical evolution of the Galaxy are those with masses greater than about 0.9 $M_\odot$. Below this limit, stars are so long lived that they have not ejected their processed material. Though flattening the IMF at low masses would affect the amount of gas trapped in stars, this can be compensated by adjusting m_{low}. A similar result was found in Scully *et al.* (1996) for models with a metallicity dependent IMF. In this case, even though a larger number of massive stars is created early on, the IMF very quickly steepens to a more normal IMF ($\varphi \sim m^{-2.6}$) so no evidence of the massive stars created early on shows up in the PDMF which results from this type of model. As these are the most extreme cases, we do not show the PDMF for the models with smaller primordial D/H.

5 Implications for ^{3}He

It is clear from the results above and from the work of Scully *et al.* 1996, that the problems concerning ^{3}He can not be fully resolved by galactic chemical evolution alone. As is well known, the root of the problem concerning ^{3}He is the production of ^{3}He in low mass stars as given for example in Eq.(25). Models in which ^{3}He is at least partially destroyed in low mass stars fare much better (Vangioni-Flam *et al.* 1994, Vangioni-Flam & Cassé 1995, Olive *et al.* 1995, and Scully *et al.* 1996) and are now being put on a firm astrophysical basis by stellar modelists themselves who invoke an extra mixing mechanism due to diffusion below the convective envelope, possibly driven by rotation (Charbonnel 1995, 1996, Hogan 1995, Wasserburg *et al.* 1995, Boothroyd & Sackman 1996, Weiss, Wagenhuber & Denissov, 1996). This mechanism seems, at the same time, to explain the high ^{13}C abundance in globular cluster red giants (see e.g. Boothroyd & Sackman (1996), for an extensive discussion). However, the important measurement of Gloeckler & Geiss (1996) leads us to reanalyze the situation.

The new measurement indicates that the sum (D + ^{3}He)/H seems to be approximately constant since the birth of the sun, varying from $4.1 \pm 0.6 \pm 1.4 \times 10^{-5}$ to $3.8 \pm 0.7 \pm 0.2 \times 10^{-5}$ (Turner *et al.* 1996). (If the measurements of D/H in Jupiter turn out to be representative

of the protosolar abundance, then (D+^{3}He)/H may actually be required to decrease over the last 4.6 Gyr.) If T_g is the galactic age in Gyr, the late ^{3}He behavior is governed by stars of lifetimes longer than $T_g - 4.6$, which corresponds to a very narrow mass range: $M(T_g)$ to $M(T_g - 4.6)$. For $T_g = 14$ Gyr, this mass range corresponds to 0.9 – 1.0 $M_\odot$. In addition, the relative constancy of the ^{3}He/H abundance from the birth of the Galaxy up to the birth of Sun would implies that above a critical mass, M_c, ($M_c > M(T_g - 4.6)$), ^{3}He is significantly destroyed. However, as noted above, the presence of a high observed ^{3}He/H abundance in planetary nebulae (Rood *et al.* 1992, 1995) indicates that not all stars can efficiently destroy ^{3}He.

Given an age of the Galaxy, T_g, once the empirical D history is fit by adjusting the essential parameters of galactic evolution, the model allows a clear empirical determination of the mass of stars which contribute to the ^{3}He enrichment from $T_g - 4.6$ Gyr until now, and also the degree of production and destruction of this isotope in different mass ranges. Stellar lifetimes are key ingredients of the model, especially those of low mass stars that arrive to maturity and shed their processed material since the birth of Solar System.

Another influential parameter, traditionally called g_3, is defined as the ^{3}He/H ratio in the ejected material divided by the initial one i.e. (D+^{3}He)/H at star formation. We have taken g_3 to be given by Eq.(25) for stars with masses less than M_c, ie. these stars are net producers of ^{3}He, while for stars more massive $M_c < M < 8M_\odot$, we have taken $g_3 = 0.1$ and for more massive stars we take g_3 from Dearborn, Schramm, & Steigman (1982). We find that in all of the cases studied, the transition mass is always $M_c \simeq 1.0$ $M_\odot$, thus the ^{3}He producers lie in a very narrow range as argued above. In figure 14, we show the evolution of D/H and ^{3}He/H for model II, assuming the above model for ^{3}He. In this case the mass cut is at 0.96 $M_\odot$.

From this analysis, a typical case emerges corresponding to $M_c \sim 1.0$ $M_\odot$ corresponding to our reference model. Below this mass, ^{3}He is produced and above it is destroyed. Thus it is expected that a few stars, in a limited mass range, do produce ^{3}He as observed in certain planetary nebulae (Rood et al 1995). Since the favorable mass range is so narrow (0.9 to 1.0 compared to that of all PN progenitors (0.9 to 8 $M_\odot$), it is not surprising that such ^{3}He rich objects are rare. Indeed, for a standard IMF we get about 17% (about 11% in the case

depicted in figure 14), which seems reasonable.

Concerning the nucleosynthesis of ^{3}He, according to our calculation, the mass of the ^{3}He-rich PN progenitors, which should have been born in the very early Galaxy, is close to 1 $M_\odot$. Unfortunately at present we can only consider such a model as empirical as it has no other real theoretical foundation. It is worth noting however, that the mass range of interest covers the region where related phenomena take place: 1) a central convective core forms which could modify the subsequent evolution (see eg. Schaller *et al.* 1992); 2) the energy production rate of the CNO cycle begins to overcome that of the p-p chain (see eg. Arnett 1996). The model above is at variance with models which invoke additional mixing in order to explain the enhanced ^{13}C abundance in red giants, and require that the bulk of the ^{3}He destruction takes place in stars with $M < 2M_\odot$. There are however several problems with the models which destroy ^{3}He only at the low end of mass function. First, there is generally not enough destruction of ^{3}He to account for the low solar ^{3}He/H abundance (Scully *et al.* 1996). Though they aid significantly, ^{3}He is still overproduced by a factor of about 2 at the solar epoch. In addition, if the progenitors of the ^{3}He rich planetary nebulae are relatively massive ($M > 2M_\odot$), then it is difficult within standard stellar models to explain the necessary enhancement of ^{3}He (^{3}He/H $\sim 10^{-3}$) in these systems (cf. Eq.(25)). The model of Boothroyd and Malaney (1996) on the other hand, does provide enough ^{3}He destruction, yet are even more problematic as far as the planetary nebulae data are concerned (Olive *et al.* 1996).

6 Conclusion

The high D/H ratio inferred from the absorbing clouds along the line of sight of certain remote quasars led us to go beyond standard galactic evolutionary schemes which can not account for a deuterium destruction factor greater than a few. To this aim, we have relaxed the closed box hypothesis and coupled a a simple galactic wind model to the galactic evolutionary one. The wind is driven by the numerous core collapse supernovae that are assumed to explode in the early galaxy, due to a somewhat enhanced massive star formation rate early on and rapidly diminishes at later times. The early generation of massive stars has three beneficial

effects: 1) they quickly eject their D-free material and induce a lowering of the D/H ratio; 2) they induce a galactic outflow as long as their explosion rate remains sufficiently high. This wind moderates the rise in metallicity; 3) they rapidly enrich the interstellar medium to such a level that the G-dwarf problem is alleviated, if not solved. With regard to the G-dwarf problem, we have emphasized that the standard excess of dwarfs at very low metallicities is largely due to the IRA. When the IRA is dropped, the problem is shifted to a *deficiency* of dwarfs at [Fe/H] ~ -0.5 and an excess at solar [Fe/H] and above. We have been able to match all of the observational constraints considered, and in particular a D destruction factor of about 10, while maintaining a solar metallicity.

The evolution of ^{3}He is more problematic and remains the least understood of the light element isotopes. We believe that the difficulty in the abundance patterns of ^{3}He resides with stellar evolution rather than with galactic chemical evolution or cosmology. Using the recent observations of Gloeckler & Geiss (1996), we have shown empirically that stars above 1.0 $M_\odot$ destroy ^{3}He thoroughly and produce it at lower masses in qualitative agreement with classical stellar evolution theory and the observations of ^{3}He in planetary nebulae.

7 Acknowledgments

We would like to thank K. Nomoto, D.N. Schramm, G. Steigman, and J.W. Truran for helpful discussions. We would especially like to thank Bernard Pagel for his helpful comments on our manuscript. This work was supported in part by PICS n°114, "Origin and evolution of the light elements," CNRS. This work was also supported in part by DOE grant DE-FG02-94ER-40823.

References

Arnett, D. 1996, *Supernovae and Nucleosynthesis* (Princeton University Press, Princeton)

Balser, D.S., Bania, T.M., Brockway, C.J., Rood, R.T., & Wilson, T.L. 1994, ApJ, 430, 667

Bazan, G. & Mathews, G.J. 1990, ApJ, 354, 644

Ben Jaffel, L. *et al.* 1996, Science, submitted

Boesgaard, A. 1996, to appear in *Formation of the Galactic Halo: Inside and Out*, eds. H. Morrison & A. Sarajedini (Astronomical Society of the Pacific Conference Proceedings)

Boothroyd, A.I. & Malaney, R.A. 1995, astro-ph/9512133

Boothroyd, A.I. & Sackman, I.-J. 1995, astro-ph/9512121

Burles, S. & Tytler, D. 1996, astro-ph/9603070

Carswell, R.F., Rauch, M., Weymann, R.J., Cooke, A.J. & Webb, J.K. 1994, MNRAS, 268, L1

Carswell, R.F., *et al.* . 1996 MNRAS, 278, 518

Charbonnel,C. 1994, A & A, 282, 811

Charbonnel,C. 1995, ApJ, 453, L41

Charlton, J. & Salpeter, E.E. 1989,

Dar, A. 1995, ApJ, 449, 550

David, L.P., Forman, W., & Jones, C. 1990, ApJ, 359, 29

Dearborn, D. S. P., Schramm, D., & Steigman, G. 1986, ApJ, 302, 35

Dearborn, D., Steigman, G. & Tosi, M. 1996, ApJ, 465, in press.

Edmunds, M.G., 1994, MNRAS, 270, L37

Edvardsson, B., Anderson, J., Gustafson, B., Lambert, D.L., Nissen, P.E., & Tomkin, J. 1993, A & A, 275, 101

Elbaz, D., Arnaud, M., & Vangioni-Flam, E. 1995, A & A, 303, 345

Fields, B.D. & Olive, K.A. 1996, Phys Lett B368, 103

Fields, B.D., Kainulainen, K., Olive, K.A., & Thomas, D. 1996 New Astronomy, in press

Francois, P., Vangioni-Flam, E., & Audouze, J. 1990, ApJ 361, 487

Galli, D., Palla, F. Ferrini, F., & Penco,U. 1995, ApJ, 433, 536

Geiss, J. 1993, in *Origin and Evolution of the Elements* eds. N. Prantzos, E. Vangioni-Flam, and M. Cassé (Cambridge:Cambridge University Press), p. 89

Gloeckler, G. & Geiss, J. 1996, Nature, 381, 210

Hartwick, F.D.A. 1976, ApJ, 209, 418

Hogan, C.J. 1995, ApJ, 441, L17

Iben, I. & Truran, J.W. 1978, ApJ, 220,980

Iben, I. & Tutukov, A. 1984, ApJ Suppl, 54, 335

Larson, R.B. 1972, Nature, 236, 21

Larson, R.B. 1974, MNRAS, 169, 229

Larson, R.B. 1986, MNRAS, 218, 409

Linsky, J.L., Brown, A., Gayley, K., Diplas, A., Savage, B. D., Ayres, T. R., Landsman, W., Shore, S. N., Heap, S. R. 1993, ApJ, 402, 694

Linsky, J.L., Diplas, A., Wood, B.E., Brown, A., Ayres, T. R., Savage, B. D., 1995, ApJ, 451, 335

Loewenstein, M. & Mushotzky, R. 1996, ApJ, 466, 695

Matteucci, F. & François, P. 1989, MNRAS, 239, 885

Mushotzky, R. *et al.* 1996, ApJ, 466, 686

Niemann, H.B. *et al.* 1996, Science, 272,846

Olive, K.A. 1986, ApJ 309, 210

Olive, K.A., Schramm, D.N., Scully, S. & Truran, J.W. 1996, in preparation

Olive, K.A., Rood, R.T., Schramm, D.N., Truran, J.W., & Vangioni-Flam, E. 1995, ApJ, 444, 680

Olive, K.A., & Scully, S.T. 1996, Int. J. Mod. Phys. A11, 409

Olive, K.A., & Steigman, G. 1995, ApJ S, 97, 49

Olive, K.A., Thielemann, F.-K., & Truran, J.W. 1987, ApJ, 313, 813

Ostriker, J.P., & Thuan, T.X. 1975, ApJ, 202, 353

Pagel, B.E.J. 1988, in *Evolutionary Phenomena in Galaxies*, ed. J. Beckman & B.E.J. Pagel (Cambridge University Press, Cambridge)

Pagel, B E.J., Simonson, E.A., Terlevich, R.J. & Edmunds, M. 1992, MNRAS, 255, 325

Rana, N.C. 1991, ARA&A, 29, 129

Reeves, H. 1991, A& A, 244, 294

Rood, R.T., Bania, T.M., & Wilson, T.L. 1992, Nature, 355, 618

Rood, R.T., Bania, T.M., Wilson, T.L., & Balser, D.S. 1995, in *the Light Element Abundances, Proceedings of the ESO/EIPC Workshop*, ed. P. Crane, (Berlin:Springer), p. 201

Rugers, M. & Hogan, C. 1996a, ApJ, 259, L1

Rugers, M. & Hogan, C. 1996b, astro-ph/9603084

Rugers, M. & Hogan, C. 1996c, in *Cosmic Abundances*, proceedings of the 6th Annual October Astrophysics Conference in Maryland, PASP conference series, in press.

Scalo, J. 1986, Fund. Cosm. Phys. 11, 1

Schaller, G., Schaerer, D., Meynet, G., & Maeder, A. 1992, A&AS, 96, 269

Schatzman, E., 1987, A&A, 172, 1

Scully, S.T. & Olive, K.A. 1995, ApJ, 446, 272

Scully, S.T., Cassé, M., Olive, K.A., Schramm, D.N., Truran, J., and Vangioni-Flam, E. 1996, ApJ, 462, 960

Songaila, A., Cowie, L.L., Hogan, C. & Rugers, M. 1994 Nature, 368, 599

Spite, F. & Spite, M. 1982, A.A., 115, 357

Talbot, R.J. & Arnett, W.D. 1973, ApJ 186, 69

Tammann, G.A. 1994, in in *Supernova, Les Houches Summer School Proceedings, Vol. 54*, ed. S. Bludman, R. Mochkovitch, & J. Zinn-Justin (Geneva: Elsevier Science Publishers), p. 1

Thielemann, F.-K., Nomoto, K. & Yokoi, K. 1986 A&A, 158, 17

Thorburn, J.A., 1994, ApJ, 421, 318

Timmes, F.X., Woosley, S.E., & Weaver, T.A. 1995, ApJSupp, 98, 617

Tinsley, B.M. 1980, Fund. Cosmic Phys., 5, 287

Truran, J.W., & Cameron, A.G.W. 1971, ApSpSci, 14, 179

Turner, M.S., Truran, J.W., Schramm, D.N., & Copi, C.J. 1996, astro-ph/9602050

Tytler, D., Fan, X.-M., and Burles, S. 1996, astro-ph/9603069

Vader, P. 1986, ApJ, 305, 669

Vangioni-Flam, E., & Audouze, J. 1988, A&A, 193, 81

Vangioni-Flam, E. & Cassé, M. 1995, ApJ, 441, 471

Vangioni-Flam, E., Olive, K.A., & Prantzos, N. 1994, ApJ, 427, 618

Vassiladis, E. & Wood, P.R. 1993, ApJ, 413, 641

Walker, T. P., Steigman, G., Schramm, D. N., Olive, K. A., & Kang, H. 1991 ApJ, 376, 51

Wampler, E.J. *et al.* . 1996, astro-ph/9512084, AA, in press

Wang, B. & Silk, J. 1993, ApJ 406, 580

Wasserburg, G.J., Boothroyd, A.I., & Sackmann, I.-J. 1995, ApJ, 447, L37

Wiedemann, V. 1977, A & A, 61, L27

Weiss, A., Wagenhuber, J., and Denissenkov, P. 1995, astro-ph/9512120

Woosley, S.E. & Weaver, T.A. 1995, ApJ Supp, 101, 55

Wyse, R., & Silk, J. 1987, ApJ, 313, L11

Yoshii, Y., Tsujimoto, T., & Nomoto, K. 1996, ApJ, 462, 266

Figure Captions

Figure 1: The evolution of D/H, and ^{3}He/H (calculated using the Iben & Truran (1978) yields) for model Ia with outflow (solid line) and without outflow (dotted line). The evolution in model II is shown by the dashed line with outflow only. Also shown are the values of these ratios at the time of the formation of the sun and today for D/H (open squares) and ^{3}He/H (filled circles).

Figure 2: The evolution of $^{16}O/^{16}O_\odot$ for model Ia with outflow (solid line), without outflow (dotted line), and model II (dashed line).

Figure 3: A comparison of the evolution of D/H and ^{3}He/H, as in Figure 1, for models Ia, Ib, and Ic.

Figure 4: A comparison of the evolution of $^{16}O/^{16}O_\odot$, as in Figure 2, for models Ia, Ib, Ic.

Figure 5: The time evolution of the outflow $o(t)$ for models Ia (solid), Ib (dotted), Ic (dot-dashed), and model II (dashed).

Figure 6: The time evolution of the total (disk) mass of the Galaxy relative to its initial mass for models Ia (solid), Ib (dotted), Ic (dot-dashed), and model II (dashed).

Figure 7: Distribution of G-dwarf stars as a function of [Fe/H] - $[Fe/H]_1$ for the simple closed box model without the IRA (solid line), and with the IRA (dashed line) ($[Fe/H]_1$ is [Fe/H] at $t = 14$ Gyr). Also plotted are the data taken from Pagel (1988).

Figure 8: Differential distribution of G-dwarf stars as a function of [Fe/H] - $[Fe/H]_1$ for the simple closed box model without the IRA (solid line), and with the IRA (dashed line) plotted against the data taken from Pagel (1988).

Figure 9: The age-metallicity relation showing $(Fe/H)/(Fe/H)_\odot$ as a function of time for the simple closed box models with (dashed) and without (solid) the IRA.

Figure 10: As in figure 7, the distribution of G-dwarf stars as a function of [Fe/H] for model Ia (solid line), model Ic (dot-dashed line), and model II (dashed line). Model Ib looks very similar to Ic on this plot.

Figure 11: As in figure 8, the differential distribution of G-dwarf stars as a function of

[Fe/H] for model Ia (solid line), model Ic (dot-dashed line) shown in a); and model II (dashed line) shown in b).

Figure 12: The age-metallicity relation showing [Fe/H] as a function of time for model Ia (solid line), model Ib (dotted line), model Ic (dot-dashed line), and model II (dashed line). The observational data taken from Edvardsson *et al.* (1993) is shown as a band.

Figure 13 Present day mass function of our model Ia as compared with the data from Scalo (1986).

Figure 14: The evolution of D/H and ^{3}He/H for model II with outflow and the Iben & Truran (1978) yields for ^{3}He (solid line) and in the same model with ^{3}He production in stars between 0.9 and 0.96 $M_\odot$ as described in section 5 (dashed line).

Figure 1

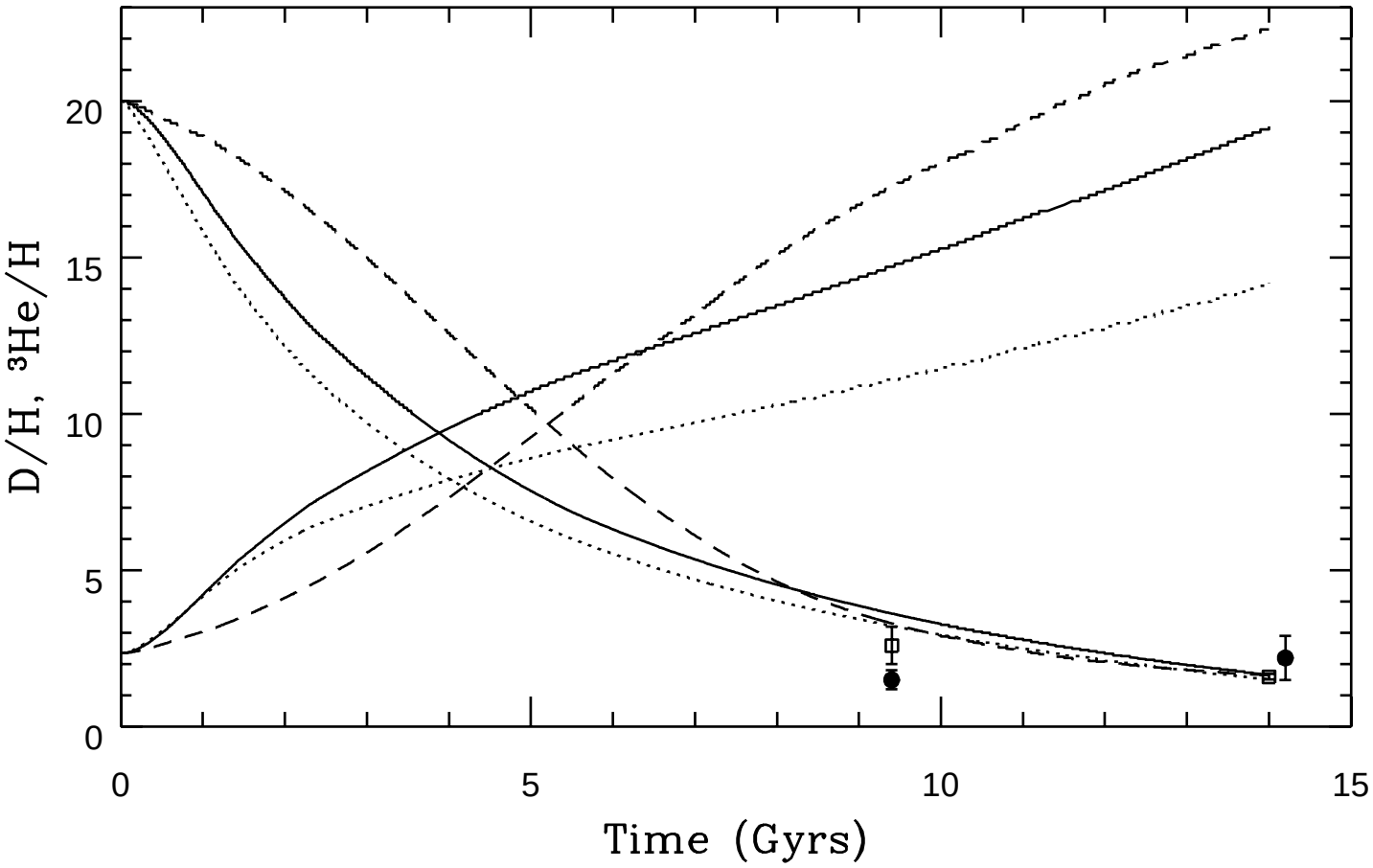

Figure 2

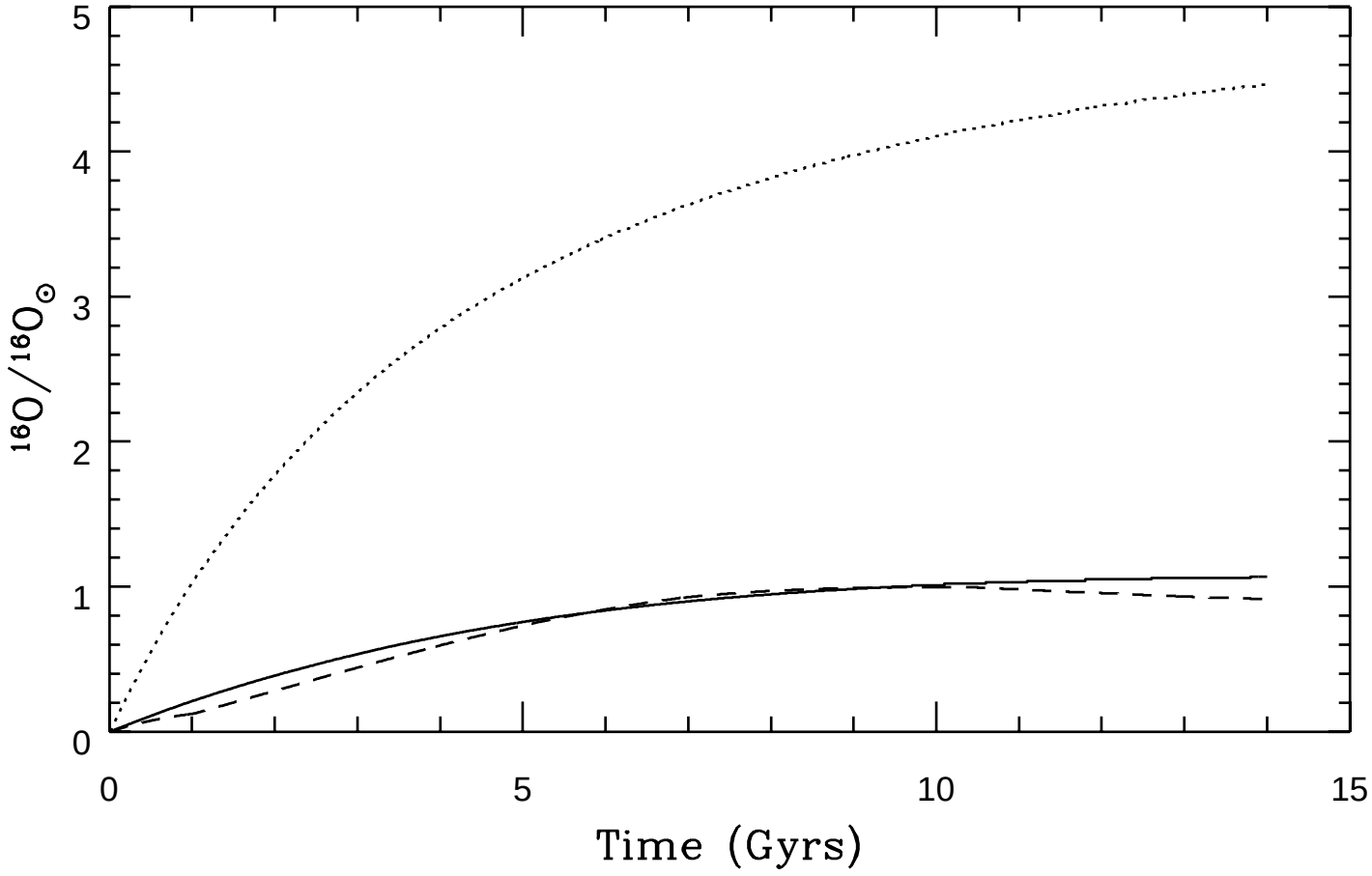

Figure 14

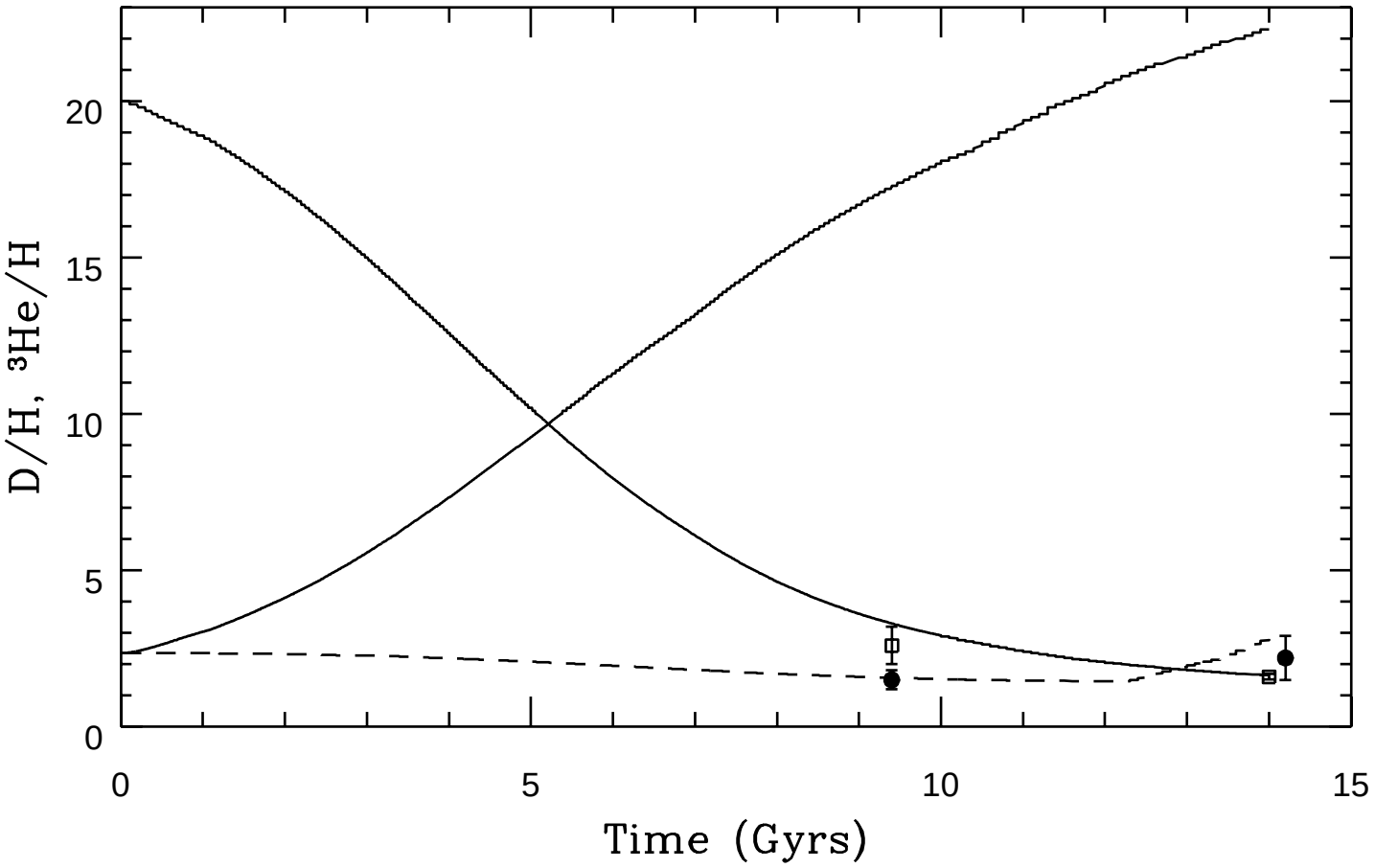

Figure 3

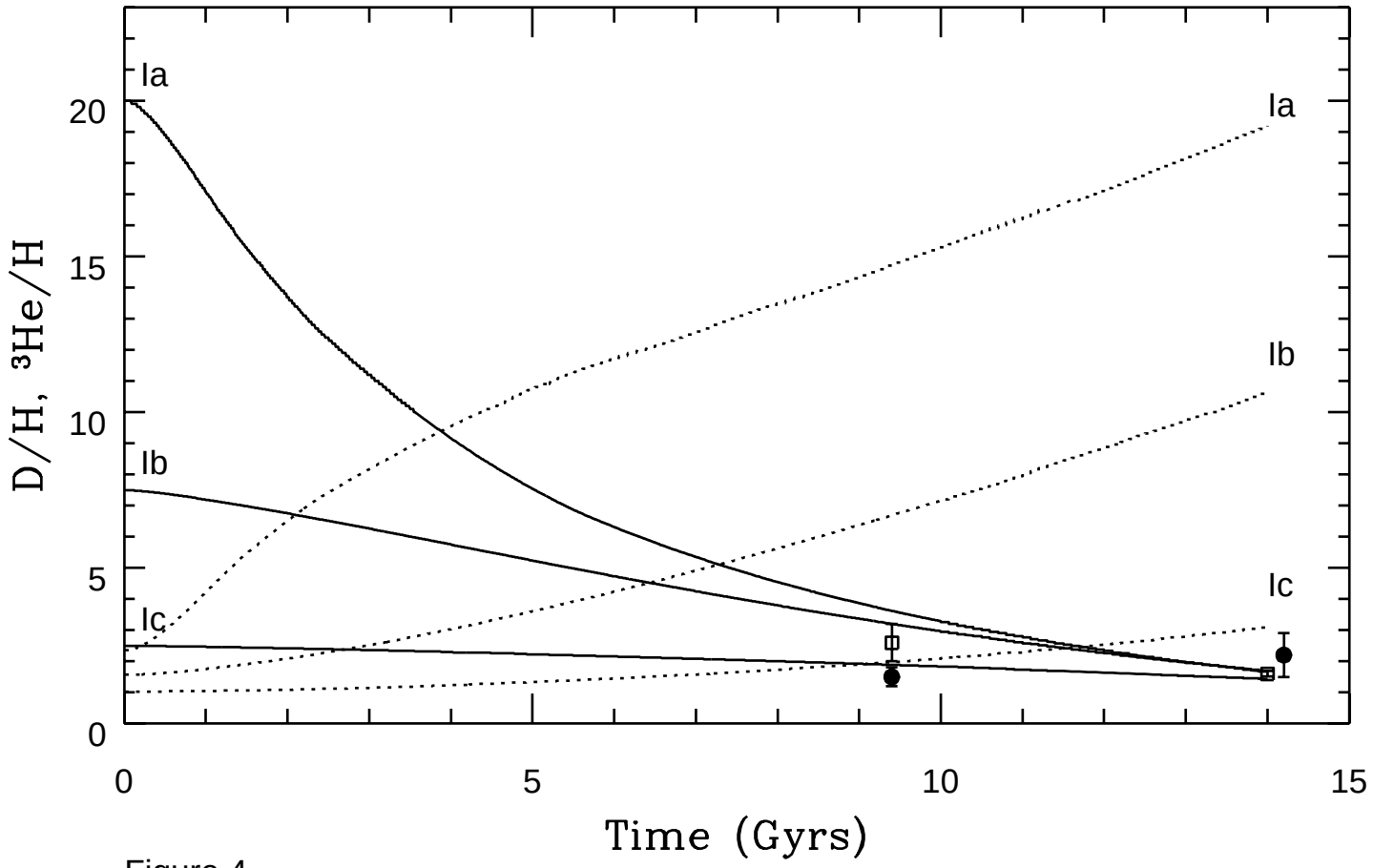

Figure 4

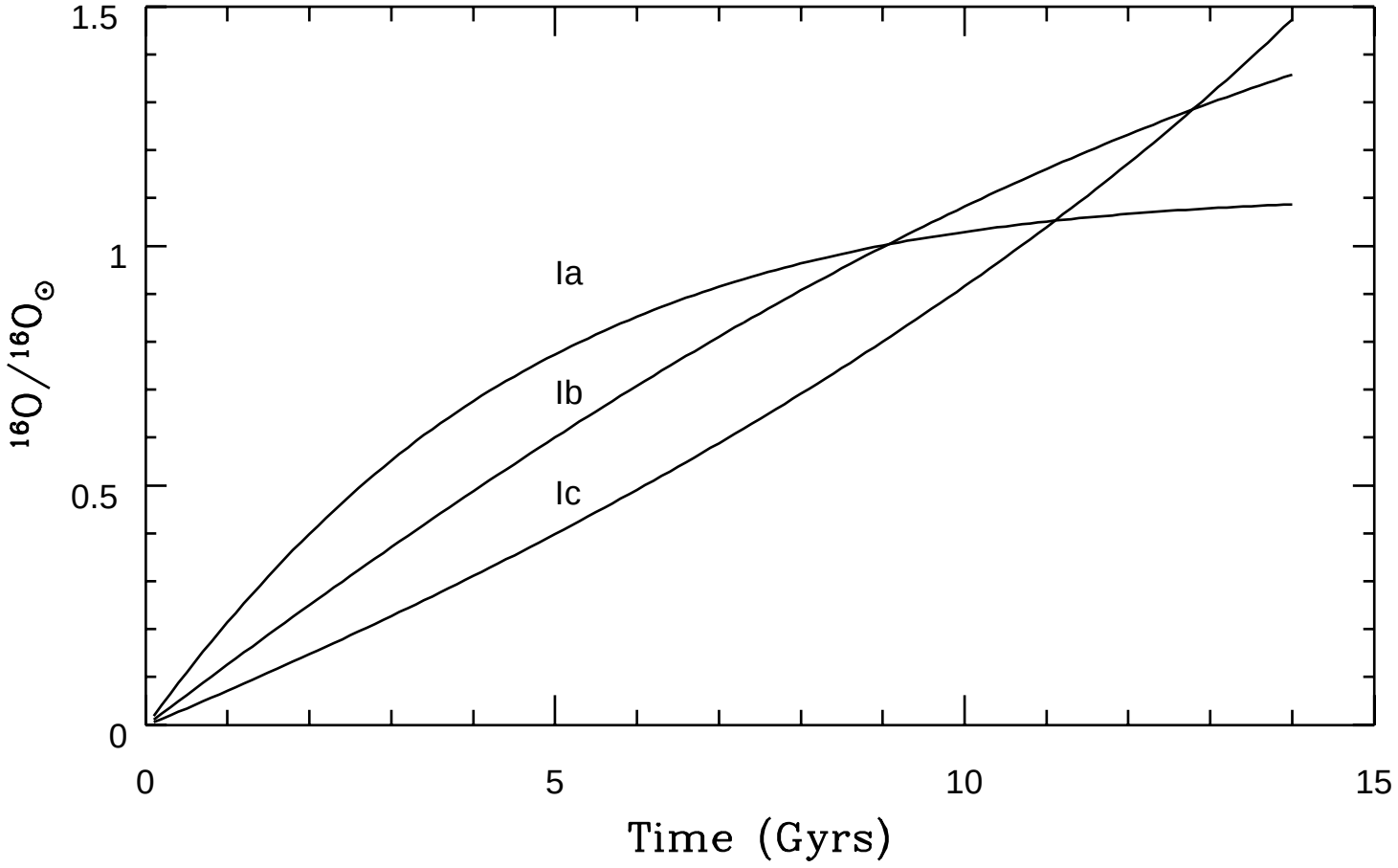

Figure 5

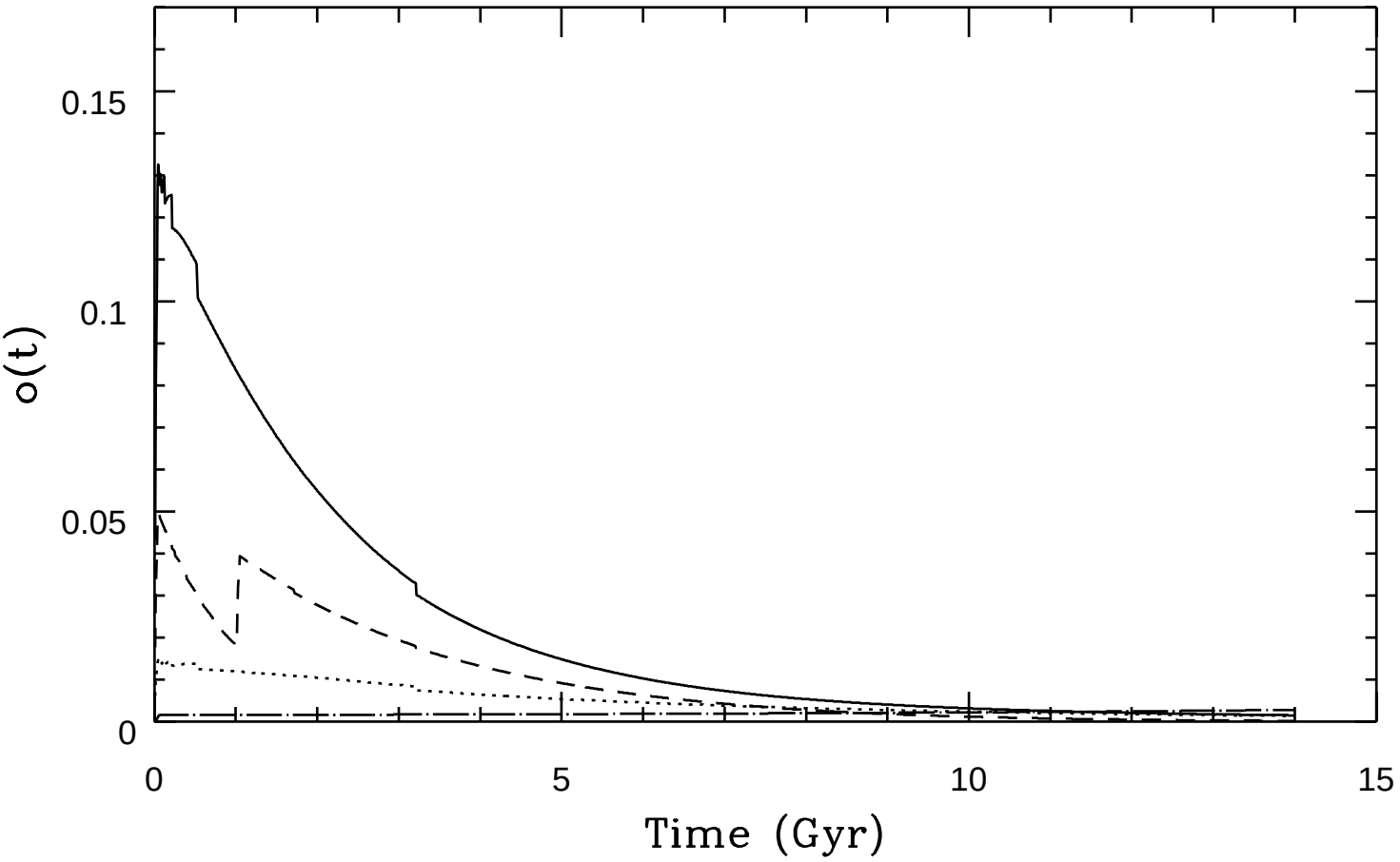

Figure 6

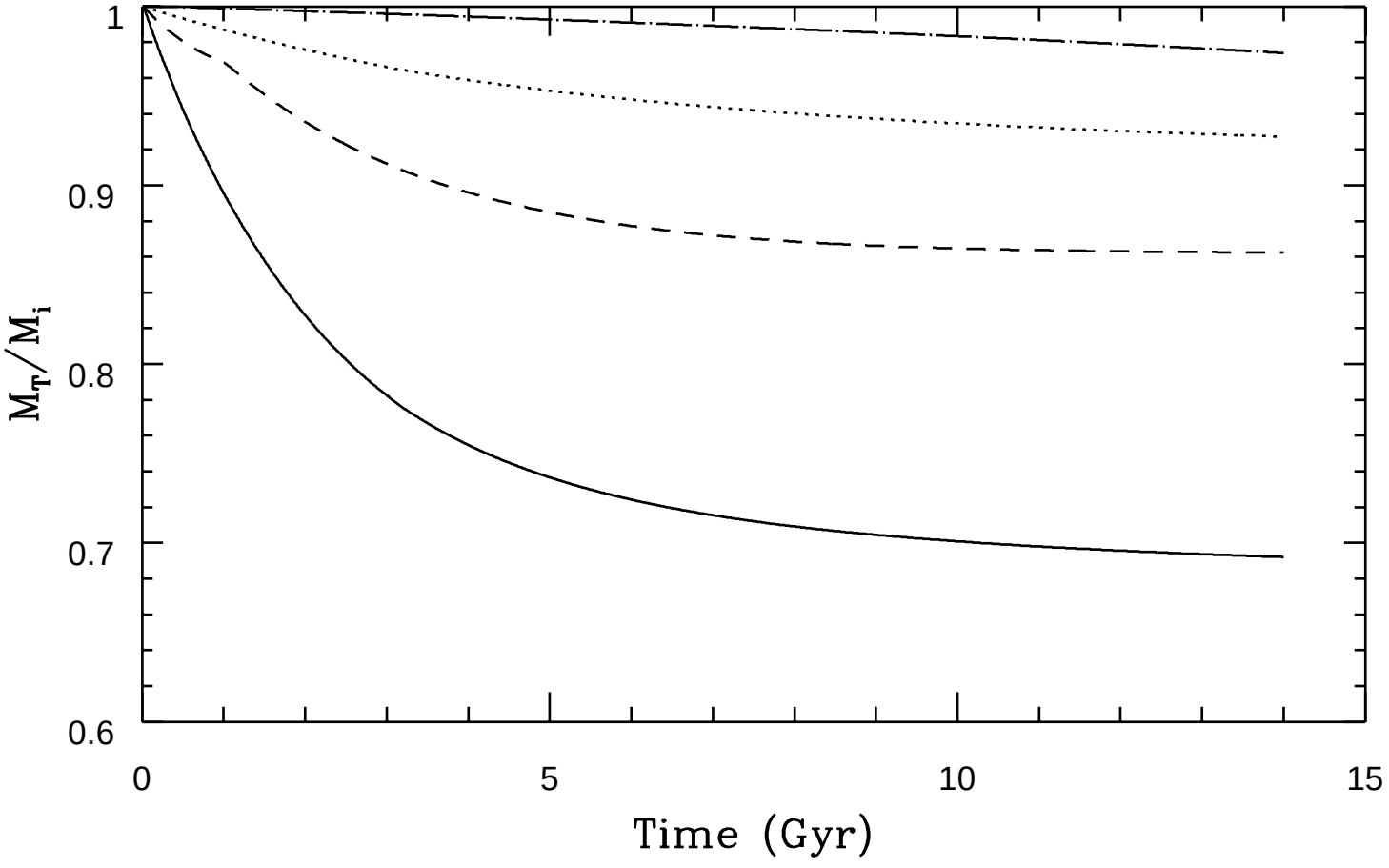

Figure 7

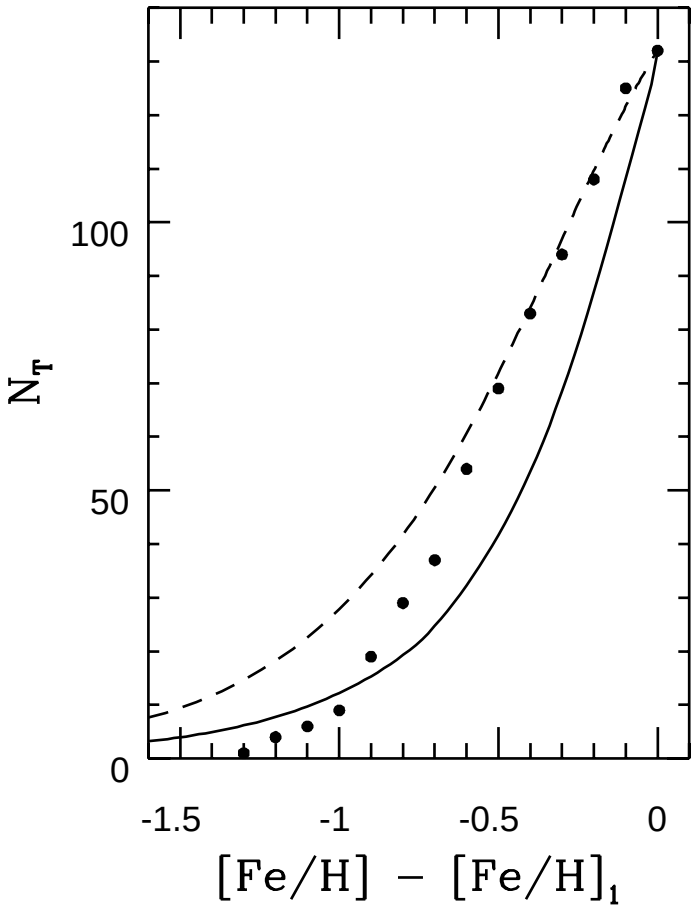

Figure 8

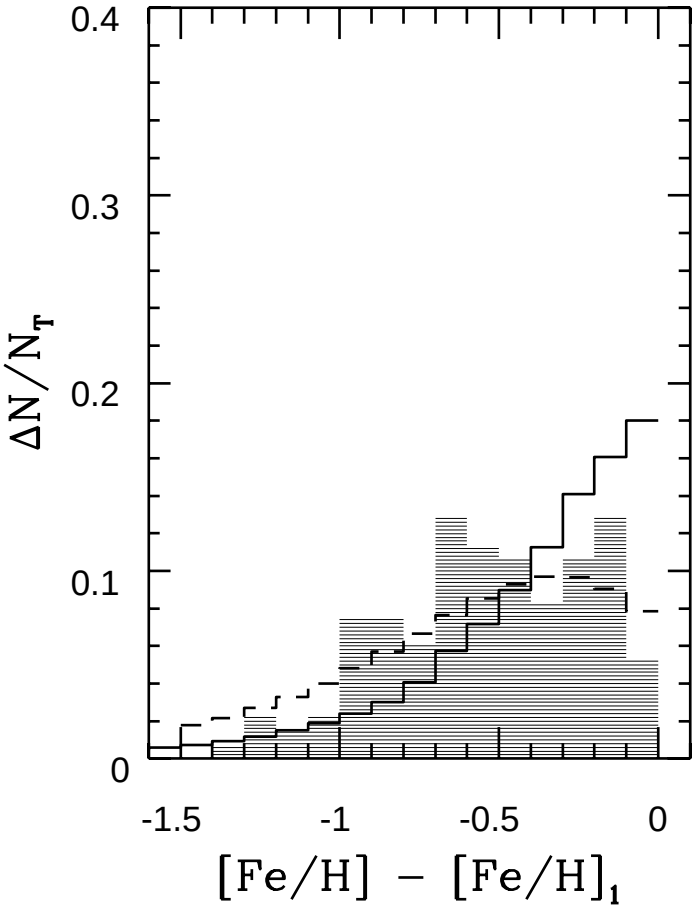

Figure 9

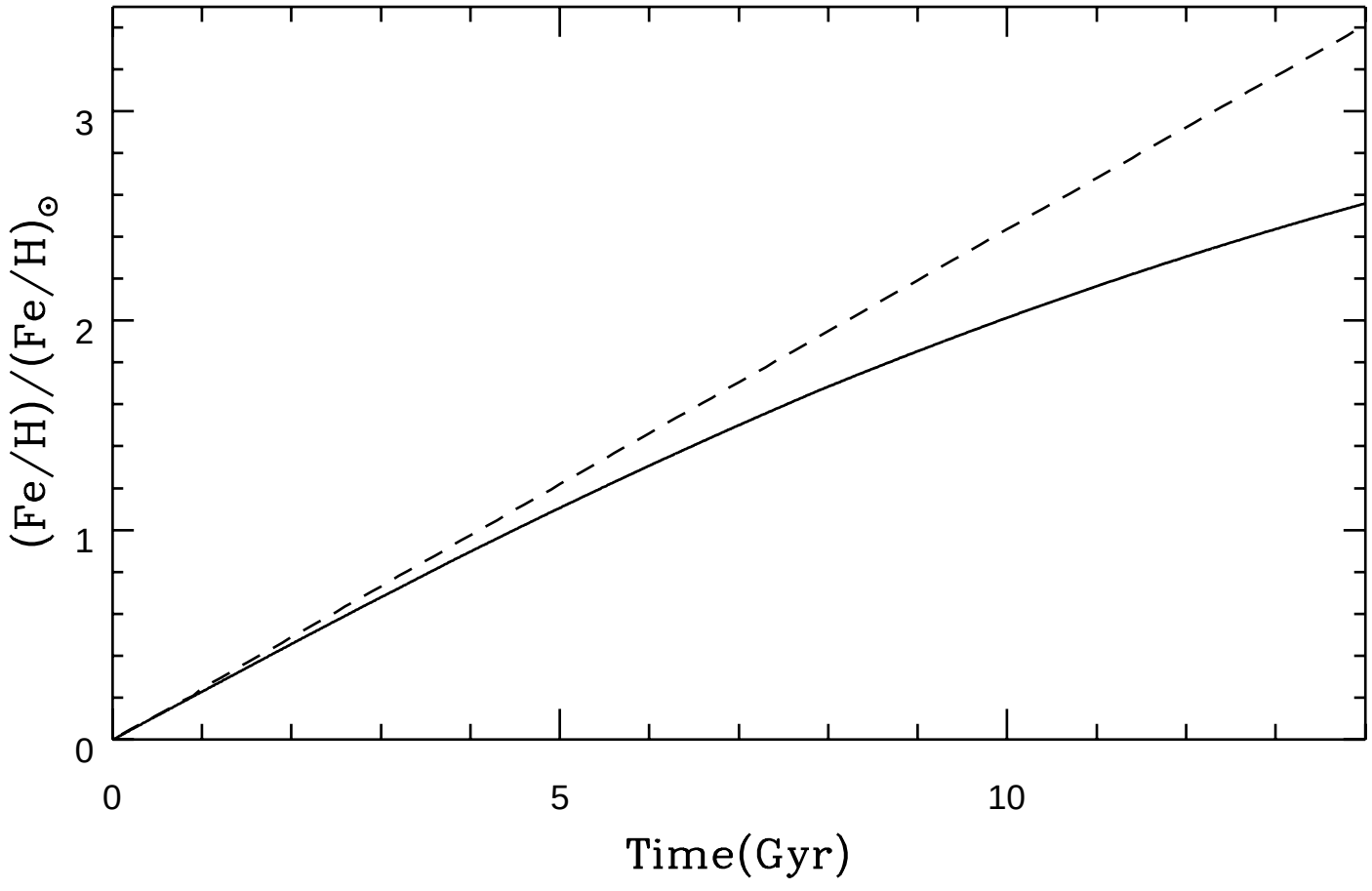

Figure 10

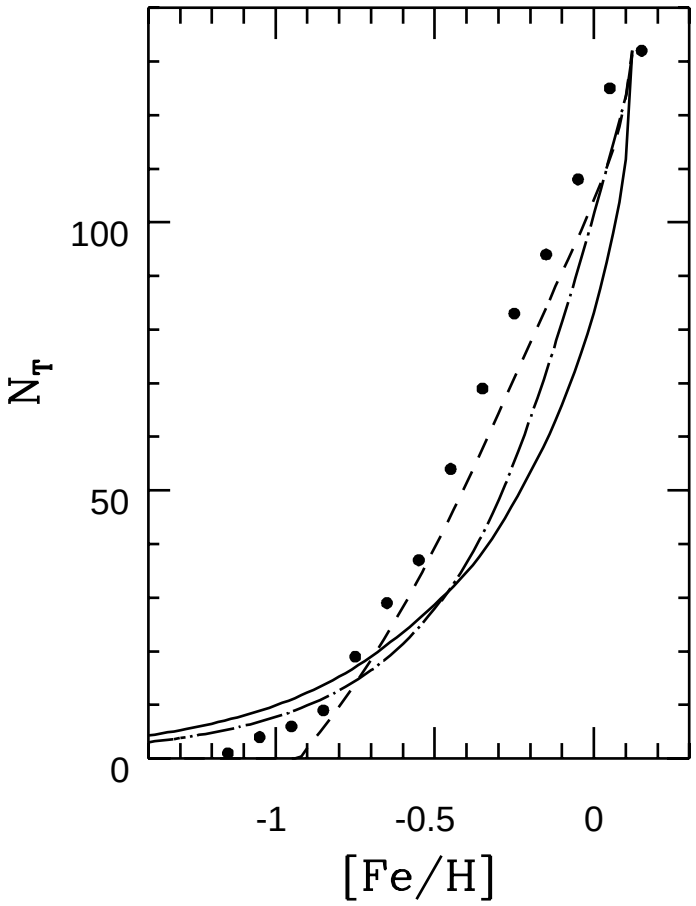

Figure 11a

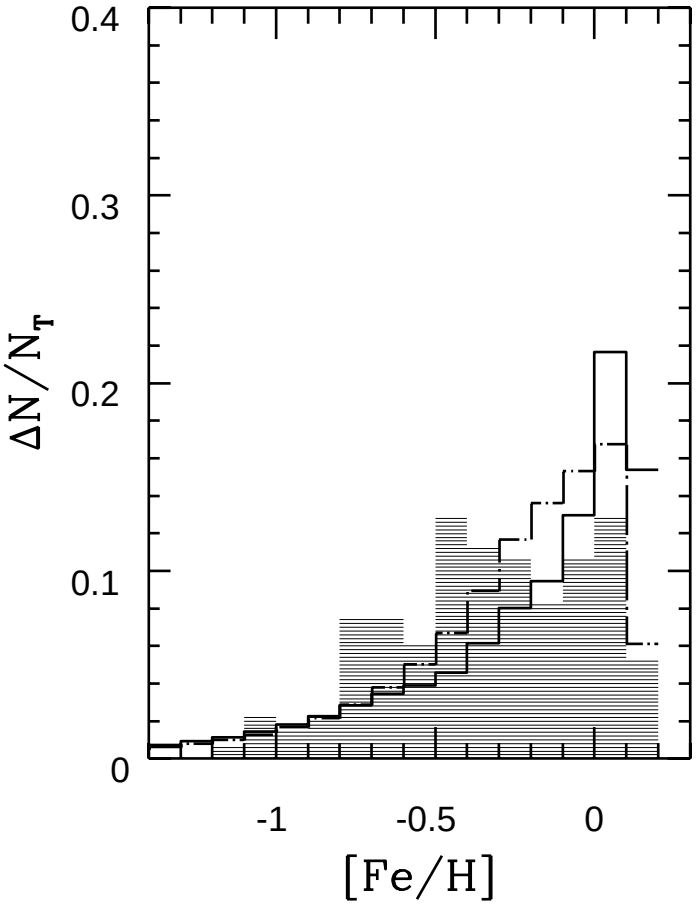

Figure 11b

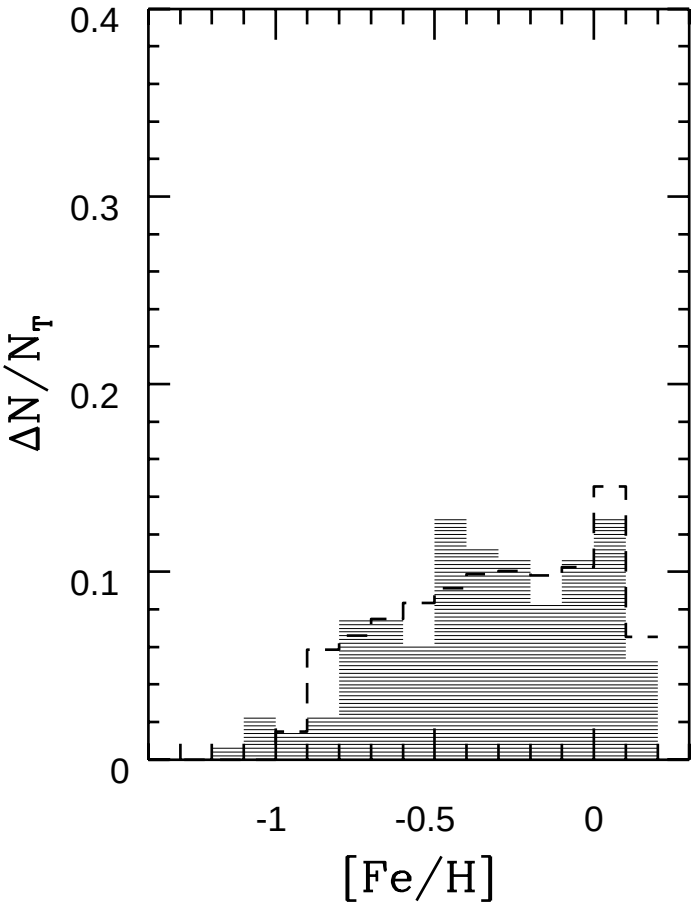

Figure 12

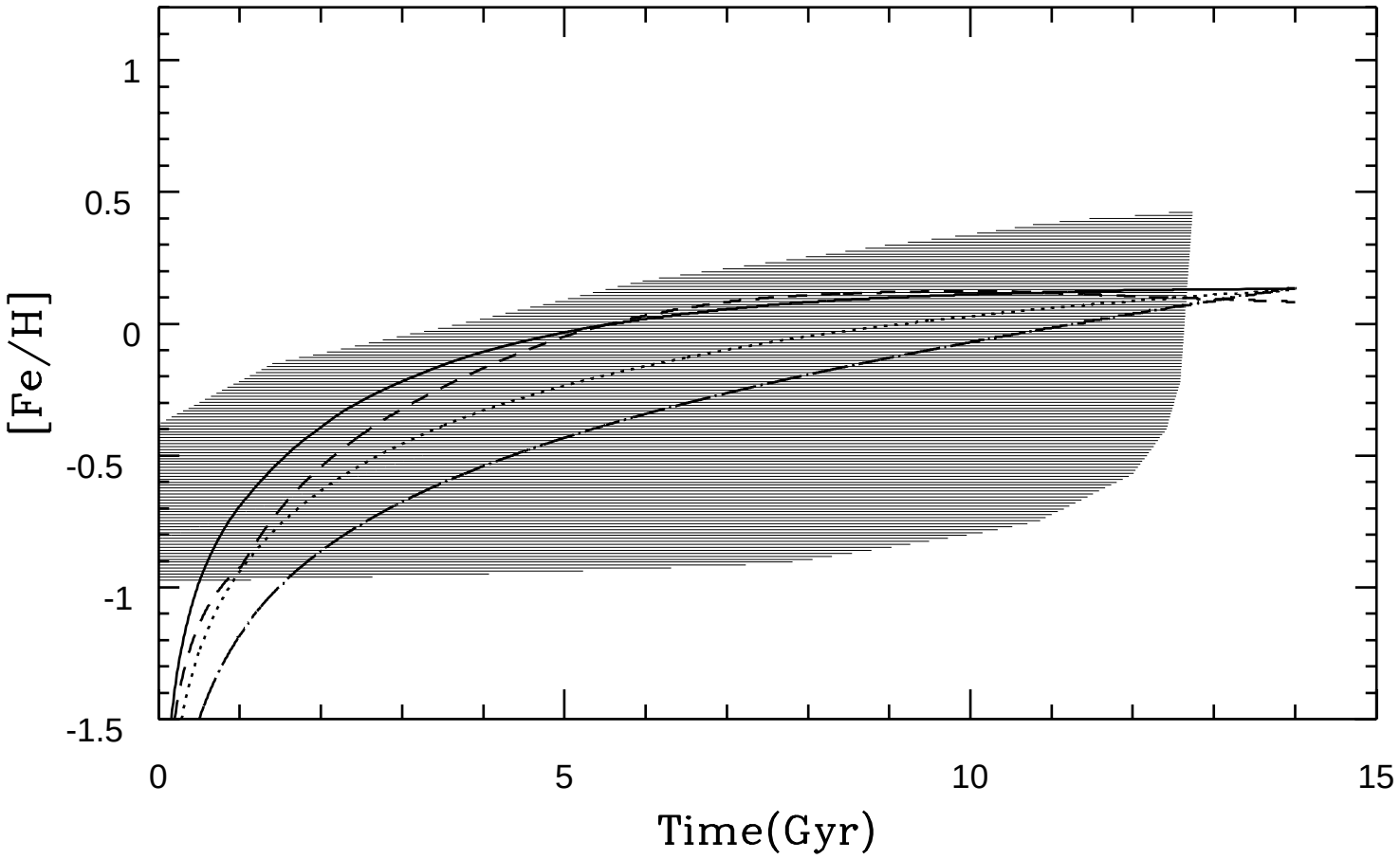

Figure 13